| *J. Exp. Zool. India* Vol. 29, No. 2, pp. 1937-1953, 2026 | DOI: https://doi.org/10.51470/jez.2026.29.2.1937 | *ISSN 0972-0030* |
|---|---|---|
| Website : www.connectjournals.com/jez | Crossref | eISSN 0976-1780 |

**ORIGINAL ARTICLE**

# BOX-BEHNKEN OPTIMIZATION AND *IN VITRO* EVALUATION OF PIPERINE-LOADED CHITOSAN NANOPARTICLES FOR SUSTAINED RELEASE, ANTI-INFLAMMATORY ACTIVITY AND HT-29 CYTOTOXICITY

**Arkadeep Misra[1], D. Suresh[2], Dilip Kumar Roy[3]*, Palash Chandra Biswas[4], A. Umadevi[5] and Victor Roychowdhury[6]**

[1,3,6]Department of Pharmaceutical Technology, JIS University, 81, Nilgunj Road, Agarpara , Kolkata - 700 109, India.
[2]KMCT College of Pharmaceutical Sciences, Kallanthode, Nitc-Po, Kozhikode - 673 601, India.
[4]Netaji Subhas Chandra Bose Institute of Pharmacy, Chakdaha - Bongaon Road, Roypara, Tatla, Nadia - 741 222, India.
[5]Department of Pharmacognosy, Vels Institute of Science, Technology and Advanced Studies, Chennai, India.
*Corresponding author e-mail : dilipk.roy@jisuniversity.ac.in; ORCID: https://orcid.org/0000-0002-3359-5501

**(Received 12 April 2026 , Revised 3 June 2026, Accepted 11 June 2026)**

**ABSTRACT : The present investigation aimed to develop and optimize piperine-loaded chitosan nanoparticles for enhanced anti-inflammatory and anticancer activity against HT-29 human colorectal cancer cells. Piperine-loaded nanoparticles were prepared using ionic gelation technique employing chitosan as polymer and sodium tripolyphosphate as crosslinking agent. A Quality by Design-based Box–Behnken Design was utilized to optimize formulation variables including chitosan concentration, TPP concentration, and Tween 80 concentration. The optimized nanoparticles were characterized for particle size, polydispersity index, zeta potential, entrapment efficiency, morphology, compatibility, crystallinity, and in vitro drug release behaviour. The optimized formulation exhibited particle size of 176.4 nm, polydispersity index of 0.241, zeta potential of +38.2 mV, and entrapment efficiency of 90.1%. FTIR, DSC and XRD studies confirmed successful encapsulation of piperine within the chitosan matrix with reduced crystallinity. Sustained drug release was observed over 24 h following diffusion-controlled kinetics. The optimized nanoparticles demonstrated significantly enhanced protein denaturation inhibition, nitric oxide scavenging activity and cytotoxicity against HT-29 cells compared with pure piperine. The $IC_{50}$ value of optimized nanoparticles was markedly lower than that of pure piperine, indicating enhanced antiproliferative efficacy. The findings suggested that chitosan-based nanoencapsulation significantly improved the pharmaceutical and biological performance of piperine for colorectal cancer therapy.**

***Key words :*** Piperine, chitosan nanoparticles, ionic gelation, Box–Behnken design, anti-inflammatory activity, HT-29 cells, colorectal cancer, cytotoxicity, sustained release, nanoparticle optimization.

**How to cite :** Arkadeep Misra, D. Suresh, Dilip Kumar Roy, Palash Chandra Biswas, A. Umadevi and Victor Roychowdhury (2026) Box-Behnken optimization and *in vitro* evaluation of piperine-loaded chitosan nanoparticles for sustained release, anti-inflammatory activity and HT-29 cytotoxicity. *J. Exp. Zool. India* **29**, 1937-1953. DOI: https://doi.org/10.51470/jez.2026.29.2.1937

## INTRODUCTION

Colorectal cancer is one of the most prevalent and life-threatening malignancies worldwide and represents a major public health burden because of its increasing incidence, high mortality rate and limitations associated with conventional chemotherapy. Despite significant advances in cancer therapeutics, currently available anticancer drugs often produce severe systemic toxicity, poor selectivity toward cancer cells, multidrug resistance, and limited therapeutic efficacy. Chronic inflammation and oxidative stress are also recognized as important contributors in colorectal carcinogenesis, tumor progression, and metastasis. Therefore, development of multifunctional therapeutic systems possessing both anti-inflammatory and anticancer properties has emerged as a promising strategy for colorectal cancer management (Abbaspour-Ravasjani *et al*, 2025; Abdelgalil *et al*, 2022; Abdelgawwad El-Sehrawy *et al*, 2025; Abuhassan *et al*, 2026).

Piperine, a naturally occurring alkaloid isolated from black pepper (*Piper nigrum*), has gained considerable scientific attention because of its broad spectrum of pharmacological activities including anti-inflammatory, antioxidant, antimicrobial, immunomodulatory, and anticancer effects. Several studies have demonstrated that piperine can inhibit cancer cell proliferation, induce

apoptosis, suppress inflammatory mediators and regulate oxidative stress pathways. Piperine has also been reported to interfere with multiple molecular signalling pathways associated with colorectal cancer progression. However, the clinical and pharmaceutical application of piperine remains significantly restricted because of its poor aqueous solubility, low oral bioavailability, rapid metabolism and limited systemic absorption. These limitations reduce its therapeutic concentration at the target site and compromise its overall biological efficacy (Talib *et al*, 2026; Tripathi *et al*, 2025; Wu *et al*, 2024; Zakaria *et al*, 2021).

Nanotechnology-based drug delivery systems have emerged as effective approaches to overcome the biopharmaceutical limitations associated with poorly soluble phytoconstituents. Among various nanocarriers, polymeric nanoparticles have attracted substantial interest because of their ability to improve drug solubility, enhance cellular uptake, provide sustained drug release, and improve therapeutic efficacy. Polymeric nanoparticles can also protect encapsulated compounds from premature degradation and facilitate controlled drug delivery to pathological tissues. Chitosan is a biodegradable, biocompatible, and mucoadhesive natural polysaccharide widely utilized in nanoparticle formulation because of its favourable pharmaceutical characteristics (Kakoti *et al*, 2016 and Kataki *et al*, 2022). The cationic nature of chitosan enables electrostatic interaction with negatively charged biological membranes, thereby enhancing cellular internalization and drug absorption. Chitosan nanoparticles additionally exhibit low toxicity, excellent biocompatibility, and inherent bioadhesive properties, making them highly suitable for anticancer drug delivery applications. Ionic gelation using sodium tripolyphosphate (TPP) is one of the most commonly employed techniques for preparation of chitosan nanoparticles because of its simplicity, mild processing conditions, and ability to produce stable nanosized systems without the use of harsh organic solvents (Das *et al*, 2023; Das *et al*, 2024; Dasuni Wasana *et al*, 2023; Dmour, 2024). Quality by Design (QbD)-based optimization approaches are increasingly applied in pharmaceutical formulation development to systematically understand the influence of formulation variables on product performance. Box–Behnken Design is an efficient statistical tool that enables optimization of multiple formulation variables with minimal experimental runs while establishing mathematical relationships between formulation factors and critical quality attributes (Darwish *et al*, 2024; Imam *et al*, 2021; Tam *et al*, 2023; Tripathi *et al*, 2026).

Considering the well-documented pharmacological potential of piperine and the advantages offered by chitosan-based nanocarriers, the present study was undertaken to develop and optimize piperine-loaded chitosan nanoparticles using the ionic gelation technique coupled with a Quality by Design (QbD)-based Box–Behnken Design approach. Although several nanoparticulate systems containing piperine have been reported, studies integrating systematic statistical optimization with comprehensive physicochemical characterization and biological evaluation remain limited. To the best of our knowledge, this is among the first studies to employ Box–Behnken Design for the optimization of piperine-loaded chitosan nanoparticles while simultaneously investigating their sustained-release behaviour, preliminary in vitro anti-inflammatory activity, and cytotoxic potential against HT-29 human colorectal cancer cells within a single formulation framework. The developed nanoparticles were comprehensively characterized for particle size, polydispersity index, zeta potential, entrapment efficiency, morphology, thermal behaviour, crystallinity, and drug release kinetics. Furthermore, their biological performance was assessed through protein denaturation inhibition, nitric oxide scavenging assays, and MTT-based cytotoxicity evaluation. The findings were intended to provide insight into the potential of optimized piperine-loaded chitosan nanoparticles as a promising in vitro drug delivery platform that warrants further preclinical investigation for colorectal cancer and inflammation-associated disorders.

## MATERIALS AND METHODS

Piperine was procured from Sigma-Aldrich and used as the active phytoconstituent for nanoparticle formulation. Chitosan (medium molecular weight, degree of deacetylation approximately 85%) was obtained from HiMedia Laboratories Pvt. Ltd. and utilized as the biodegradable polymeric carrier. Sodium tripolyphosphate (TPP), employed as the ionic crosslinking agent, was purchased from Merck Life Science Pvt. Ltd. Tween 80 and glacial acetic acid were obtained from Loba Chemie Pvt. Ltd. and Merck Life Science Pvt. Ltd., respectively. Ethanol of analytical grade was used as the solvent for piperine solubilization. Dulbecco's Modified Eagle Medium (DMEM), fetal bovine serum (FBS), penicillin–streptomycin solution, phosphate-buffered saline (PBS), and trypsin-EDTA were procured from Gibco, Thermo Fisher Scientific for cell culture studies. MTT reagent, bovine serum albumin, and Griess reagent components were purchased from Sigma-Aldrich. Diclofenac sodium was used as the reference anti-inflammatory standard. All reagents and chemicals employed in the study were of analytical grade and used without further purification.

Double-distilled water was utilized throughout the experimental work.

## Experimental design and Optimization strategy

The formulation and optimization of piperine-loaded chitosan nanoparticles were performed using a Quality by Design (QbD)-based statistical optimization approach employing Box–Behnken Design (BBD). The experimental design was generated using Design-Expert Software Version 13. Three independent formulation variables were selected based on preliminary screening studies, including chitosan concentration (A), sodium tripolyphosphate concentration (B), and Tween 80 concentration (C). Each factor was studied at three levels designated as low (1), medium (0), and high (+1). The selected dependent responses included particle size (Y1), entrapment efficiency (Y2), cumulative drug release at 24 h (Y3), and zeta potential (Y4). A total of seventeen experimental runs comprising twelve factorial points and five center points were generated by the software. The optimization objective was to minimize particle size while maximizing entrapment efficiency, zeta potential, and sustained drug release behaviour (Waghule *et al*, 2021; Yadha *et al*, 2024; Zeeshan *et al*, 2023).

## Preliminary Screening of Formulations

Preliminary formulation trials were conducted to identify the suitable polymer-crosslinker ratio for nanoparticle formation. Six different formulations were prepared by varying the concentrations of chitosan and TPP while maintaining a constant amount of piperine. The prepared formulations were visually examined for aggregation, phase separation, nanosuspension stability, and particle formation efficiency. Formulations exhibiting particle sizes below 250 nm, acceptable dispersity and high entrapment efficiency were selected for further optimization using Box–Behnken Design (Elshazly *et al*, 2025; Kalpana *et al*, 2025).

## Preparation of Piperine-Loaded Chitosan nanoparticles

Piperine-loaded chitosan nanoparticles were prepared using the ionic gelation method. Chitosan solution was prepared by dissolving the required quantity of chitosan in 1% v/v aqueous acetic acid solution under continuous magnetic stirring overnight to obtain a clear polymeric solution. Separately, piperine was dissolved in ethanol to form a homogeneous drug solution. Tween 80 was incorporated into the chitosan solution as a stabilizing surfactant. The piperine solution was slowly added into the chitosan solution under continuous stirring at 1000 rpm. Subsequently, aqueous sodium tripolyphosphate solution was added dropwise into the polymer-drug dispersion under constant magnetic stirring. Ionic interaction between positively charged amino groups of chitosan and negatively charged phosphate groups of TPP resulted in spontaneous formation of nanoparticles. The obtained nanosuspension was subjected to probe sonication for 5 min to reduce particle aggregation and improve uniformity. The dispersion was centrifuged at 15,000 rpm for 30 min at 4°C using a refrigerated centrifuge. The separated nanoparticles were washed twice with distilled water to remove unentrapped drug and excess reagents. Mannitol (3% w/v) was added as a cryoprotectant prior to lyophilization. The final nanoparticles were freeze-dried and stored in airtight containers for further characterization studies (Tan *et al*, 2024; Yadav *et al*, 2024; Zaghloul *et al*, 2022; Zainol Abidin *et al*, 2023).

## Characterization of Piperine-loaded Chitosan nanoparticles

**Analytical method Validation for Piperine estimation :** Quantitative estimation of piperine in entrapment efficiency and in vitro drug release studies was performed using a UV–Visible spectrophotometric method. The analytical method was validated according to ICH Q2(R2) guidelines with respect to linearity, accuracy, precision, limit of detection (LOD) and limit of quantification (LOQ). A standard stock solution of piperine was prepared in ethanol and subsequently diluted to obtain concentrations ranging from 2–20 µg/mL. The absorbance of each solution was measured at 342 nm against a suitable blank. Calibration curves were constructed by plotting absorbance against concentration, and regression analysis was performed to determine linearity. Precision was evaluated through repeatability studies and expressed as percentage relative standard deviation (%RSD). Accuracy was assessed using recovery studies at different concentration levels. LOD and LOQ were calculated using the standard deviation of the response and slope of the calibration curve according to ICH recommendations.

**Particle size, Polydispersity Index and Zeta potential :** The average particle size, polydispersity index (PDI), and zeta potential of the prepared nanoparticles were determined using dynamic light scattering technique with a Malvern Zetasizer Nano ZS90. The nanoparticle suspension was appropriately diluted with double-distilled water prior to analysis to avoid multiple scattering effects. Measurements were performed at 25°C and all readings were recorded in triplicate. Mean particle size was expressed in nanometers, while zeta potential values were expressed in millivolts (Abd El-Hadi, 2025; Tan *et al*, 2024; Yadav *et al*, 2024; Zaghloul *et al*, 2022; Zainol

Abidin *et al*, 2023).

**Determination of Entrapment efficiency :** Entrapment efficiency of piperine-loaded nanoparticles was determined by indirect centrifugation method. The nanoparticle suspension was centrifuged at 15,000 rpm for 30 min, and the supernatant containing free unentrapped drug was collected. The amount of free piperine present in the supernatant was analyzed spectrophotometrically at 342 nm using a UV-visible spectrophotometer. The entrapment efficiency was calculated using the following equation (Tan *et al*, 2024; Yadav *et al*, 2024; Zaghloul *et al*, 2022; Zainol Abidin *et al*, 2023):

$$EE(\%) = \frac{Total\ Drug - Free\ Drug}{Total\ Drug} \times 100$$

Drug loading was determined to evaluate the amount of piperine successfully incorporated within the nanoparticle matrix relative to the total weight of nanoparticles obtained. The drug loading percentage was calculated using the following equation:

$$\text{Drug Loading (\%)} = \frac{Entrapped\ Drug}{Total\ Nanoparticle\ Weight} \times 100$$

All measurements were carried out in triplicate and the results were expressed as mean ± standard deviation.

**Surface Morphology by Scanning Electron Microscopy :** Surface morphology of the optimized nanoparticle formulation was evaluated using scanning electron microscopy (SEM). The lyophilized nanoparticle sample was mounted on an aluminium stub using double-sided adhesive carbon tape and coated with a thin layer of gold under vacuum. The samples were examined at different magnifications to evaluate particle shape, surface characteristics, and aggregation behaviour (Tan *et al*, 2024; Yadav *et al*, 2024; Zaghloul *et al*, 2022; Zainol Abidin *et al*, 2023).

**Fourier Transform Infrared Spectroscopy (FTIR) :** FTIR analysis was performed to investigate possible interactions between piperine and formulation excipients. FTIR spectra of pure piperine, chitosan, TPP, physical mixture, and optimized nanoparticles were recorded using an FTIR spectrophotometer within the scanning range of 4000–400 $cm^{-1}$ employing potassium bromide pellet method. The obtained spectra were analyzed for characteristic functional group peaks and possible peak shifting or disappearance.

**Differential Scanning Calorimetry (DSC) :** Thermal behaviour of pure drug, polymer and optimized nanoparticles was evaluated using differential scanning calorimetry. Approximately 5 mg of each sample was sealed in aluminium pans and heated over a temperature range of 30–300°C at a heating rate of 10°C/min under nitrogen atmosphere. Thermograms were analyzed to assess crystallinity changes and drug encapsulation within the nanoparticle matrix.

**X-Ray Diffraction (XRD) :** X-ray diffraction analysis was performed to determine the crystalline characteristics of piperine before and after nanoparticle formulation. Powder samples were scanned over a diffraction angle range of 5°–60° (2θ) using an X-ray diffractometer. Changes in diffraction intensity and peak sharpness were evaluated to determine amorphization and molecular dispersion of piperine within the polymeric system.

***In vitro* Drug Release study**

The *in vitro* release behaviour of piperine from the optimized chitosan nanoparticles was evaluated using the dialysis bag diffusion technique. A pre-soaked dialysis membrane having a molecular weight cut-off of 12,000–14,000 Da was used for the study. An accurately weighed quantity of piperine-loaded nanoparticles equivalent to 10 mg of piperine was dispersed in a small volume of phosphate-buffered saline and transferred into the dialysis bag, which was securely tied at both ends. The dialysis bag was immersed in 100 mL of phosphate-buffered saline (PBS, pH 7.4) maintained at 37 ± 0.5°C under continuous magnetic stirring at 100 rpm. At predetermined time intervals of 0.5, 1, 2, 4, 6, 8, 12 and 24 h, 2 mL aliquots were withdrawn from the dissolution medium and replaced immediately with equal volumes of fresh buffer to maintain sink conditions. The amount of piperine released was quantified spectrophotometrically at 342 nm using a UV-visible spectrophotometer. All experiments were carried out in triplicate, and cumulative percentage drug release was calculated and expressed as mean ± standard deviation (Tan *et al*, 2024; Yadav *et al*, 2024; Zaghloul *et al*, 2022; Zainol Abidin *et al*, 2023).

**Drug Release Kinetics**

The *in vitro* release data obtained from the optimized nanoparticle formulation were fitted into different kinetic models to elucidate the mechanism of drug release. The release profiles were analyzed according to zero-order, first-order, Higuchi and Korsmeyer–Peppas kinetic models.

The mathematical expressions used for release kinetic analysis were as follows:

Zero-Order Model

$$Q_t = Q_0 + k_0 t$$

where, $Q_t$ represents the amount of drug released at time t, $Q_0$ is the initial amount of drug and $k_0$ is the zero-order release constant.

First-Order Model

$$\log Q_t = \log Q_0 - \frac{k_1 t}{2.303}$$

where, $k_1$ represents the first-order release constant.

Higuchi Model

$$Q = k_H t^{1/2}$$

where, $Q$ is the cumulative amount of drug released and $k_H$ is the Higuchi dissolution constant.

Korsmeyer–Peppas Model

$$\frac{M_t}{M_\infty} = kt^n$$

where, $M_t/M_\infty$ represents fractional drug release, $k$ is the kinetic constant and $n$ is the release exponent indicative of the release mechanism. The coefficient of determination ($R^2$) values obtained from each model were compared to identify the best-fit release kinetics.

### *In vitro* Anti-inflammatory activity

**Protein Denaturation Inhibition assay :** The anti-inflammatory activity of pure piperine and optimized piperine-loaded chitosan nanoparticles was evaluated using inhibition of protein denaturation method employing bovine serum albumin as the protein source. Different concentrations of the samples ranging from 25–200 µg/mL were prepared in phosphate-buffered saline. Diclofenac sodium served as the reference standard. To each test tube, 0.45 mL of bovine serum albumin solution and 0.05 mL of sample solution were added and incubated at room temperature for 20 min. The reaction mixtures were subsequently heated at 57°C for 3 min and allowed to cool. The absorbance was measured at 660 nm using a UV-visible spectrophotometer. The percentage inhibition of protein denaturation was calculated using the following equation (Abbas *et al*, 2026; Abbas *et al*, 2024; Abd El Hady Mousa *et al*, 2021; Kataki *et al*, 2014):

$$\%\, Inhibition = \frac{A_c - A_t}{A_c} \times 100$$

where, $A_c$ represents absorbance of the control and At represents absorbance of the test sample.

All experiments were conducted in triplicate and results were expressed as mean ± standard deviation.

**Nitric Oxide Scavenging assay :** Nitric oxide scavenging activity of the prepared nanoparticles was evaluated using sodium nitroprusside and Griess reagent method. Different concentrations of pure piperine and optimized nanoparticles were prepared within the range of 25–200 µg/mL. Sodium nitroprusside solution in phosphate-buffered saline was mixed with sample solutions and incubated at 25°C for 150 min under light exposure. After incubation, an equal volume of Griess reagent was added to the reaction mixture. The absorbance of the resulting chromophore was measured spectrophotometrically at 546 nm. Diclofenac sodium was used as the reference standard. The percentage nitric oxide scavenging activity was calculated using the standard inhibition equation. All determinations were performed in triplicate (Ahalya *et al*, 2026; Dharmalingam *et al*, 2025; Kataki, 2010).

### *In vitro* Cytotoxicity study on HT-29 cells

**Cell Culture conditions :** Human colorectal adenocarcinoma HT-29 cells were procured from a certified cell repository (NCCS Pune) and cultured in Dulbecco's Modified Eagle Medium supplemented with 10% fetal bovine serum and 1% penicillin–streptomycin solution. The cells were maintained in a humidified $CO_2$ incubator at 37°C with 5% $CO_2$ atmosphere. Subculturing was carried out using trypsin-EDTA solution upon reaching approximately 80% confluency.

**MTT Cytotoxicity assay :** The cytotoxic potential of pure piperine, blank nanoparticles, and optimized piperine-loaded chitosan nanoparticles was evaluated using MTT assay. HT-29 cells were seeded into 96-well plates at a density of $1 \times 10^4$ cells/well and incubated for 24 h to allow cell attachment. Following incubation, the cells were treated with different concentrations of formulations ranging from 12.5–200 µg/mL and further incubated for 24 h. Untreated cells served as negative control, while blank nanoparticles were used to evaluate polymer-associated cytotoxicity. After treatment, MTT reagent solution was added to each well and incubated for 4 h at 37°C. The formed purple formazan crystals were dissolved using dimethyl sulfoxide, and absorbance was measured at 570 nm using a microplate reader. Cell viability percentage was calculated using the following equation (Abbas *et al*, 2022; Abiodun *et al*, 2022; Abolhasanzadeh *et al*, 2024):

$$\%\, Cell\ Viability = \frac{Absorbance\ of\ treated\ cells}{Absorbance\ of\ control\ cells} \times 100$$

The $IC_{50}$ values for pure piperine and optimized nanoparticles were determined from dose-response curves. All experiments were performed in triplicate.

## Statistical analysis

All experimental data were expressed as mean ± standard deviation (SD) for three independent experiments (n = 3). Statistical analysis was performed using GraphPad Prism 10. Comparisons among groups were carried out using one-way analysis of variance (ANOVA) followed by Tukey's post hoc test. Statistical significance was considered at $p < 0.05$. The experimental design data generated from Box–Behnken Design were analyzed using Design-Expert Version 13 software to establish polynomial equations, response surface plots, contour plots, and desirability optimization models.

# RESULTS AND DISCUSSION

## Validation of UV Spectrophotometric method

The UV spectrophotometric method developed for piperine estimation demonstrated excellent linearity within the concentration range of 2–20 µg/mL. The calibration curve exhibited a strong linear relationship between concentration and absorbance with a correlation coefficient ($R^2$) of 0.9993. The method showed satisfactory precision with %RSD values below 2%, indicating good repeatability. Recovery studies demonstrated accuracy within the acceptable range of 98–102%, confirming the reliability of the analytical procedure. The calculated LOD and LOQ values indicated adequate sensitivity for quantification of piperine during entrapment efficiency and in vitro release studies. The results confirmed that the developed method was suitable for routine quantitative estimation of piperine in nanoparticle formulations.

## Preliminary Screening of Piperine-Loaded Chitosan Nanoparticles

Six preliminary formulations were prepared to identify the appropriate concentration range of chitosan and TPP required for stable nanoparticle formation. The formulations were evaluated based on visual appearance, nanosuspension stability, particle size and entrapment efficiency. Formulations containing lower polymer concentration exhibited reduced entrapment efficiency because of insufficient matrix formation, whereas excessively high polymer concentrations resulted in increased viscosity and particle aggregation. Formulations F3–F5 demonstrated comparatively better nanosuspension stability, smaller particle size, and higher entrapment efficiency, indicating their suitability for further optimization through Box–Behnken Design.

The reduction in particle size observed from F1 to F4 may be attributed to efficient ionic interaction between chitosan and TPP, resulting in compact nanoparticle formation. However, excessive polymer concentration in

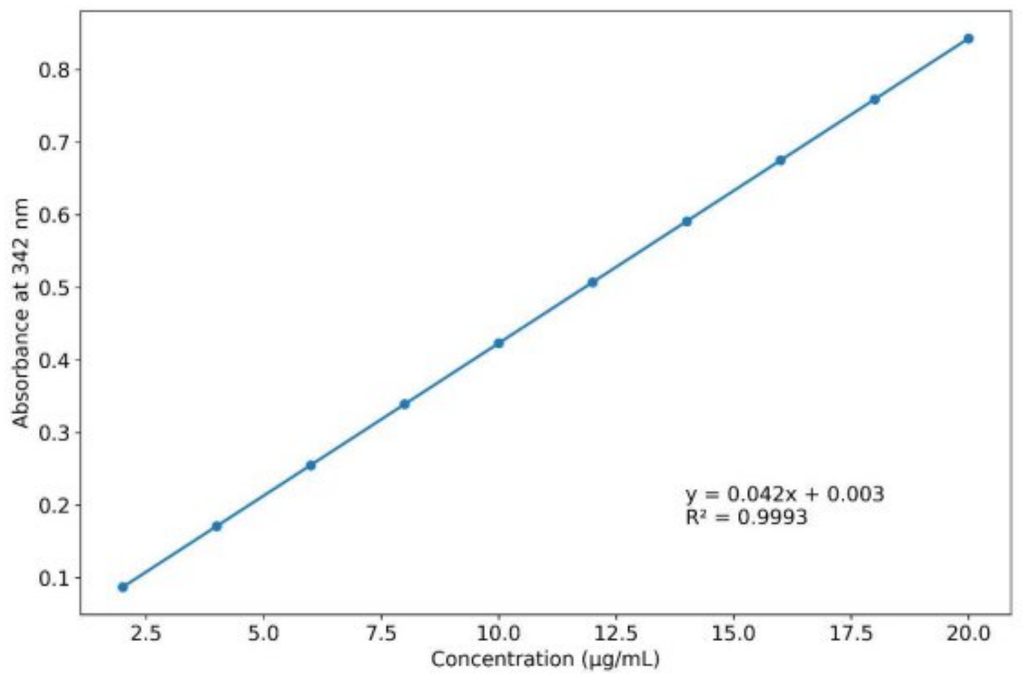


**Fig. 1 :** Calibration curve of piperine at 342 nm showing linearity over the concentration range of 2–20 µg/mL.

**Table 1 :** Validation Parameters of UV Spectrophotometric Method for Piperine.

| Parameter | Result |
|---|---|
| $\lambda_{max}$ | 342 nm |
| Linearity Range | 2–20 µg/mL |
| Regression Equation | y = 0.042x + 0.003 |
| Correlation Coefficient ($R^2$) | 0.9993 |
| LOD | 0.18 µg/mL |
| LOQ | 0.55 µg/mL |
| Accuracy (Recovery) | 98.7-101.2% |
| Precision (%RSD) | < 2.0% |

F6 increased viscosity and promoted particle aggregation, leading to larger particle size and broader size distribution. Similar observations have been reported in chitosan nanoparticle systems where optimal polymer-crosslinker balance governs nanoparticle compactness and colloidal stability.

## Optimization using Box–Behnken Design

A three-factor, three-level Box–Behnken Design consisting of 17 experimental runs was employed to optimize the nanoparticle formulation variables. Chitosan concentration (A), TPP concentration (B), and Tween 80 concentration (C) were selected as independent variables. The responses studied included particle size, entrapment efficiency, cumulative drug release at 24 h, and zeta potential.

The observed responses demonstrated that increasing chitosan concentration significantly improved entrapment efficiency and zeta potential because of enhanced polymeric matrix formation and increased surface amino groups. However, excessive polymer concentration produced larger particle sizes due to elevated viscosity during nanoparticle formation. Tween 80 effectively reduced interfacial tension and improved nanoparticle uniformity, thereby reducing particle size. The optimized formulation corresponded to Run 12, which exhibited

**Table 2 :** Preliminary Screening formulations and Physicochemical evaluation.

| Formulation | Particle Size (nm) | PDI | Zeta Potential (mV) | Entrapment Efficiency (%) |
|---|---|---|---|---|
| F1 | 312.5 ± 8.4 | 0.521 ± 0.02 | +18.4 ± 1.2 | 58.6 ± 2.1 |
| F2 | 268.7 ± 6.2 | 0.446 ± 0.01 | +21.2 ± 1.4 | 66.3 ± 1.8 |
| F3 | 214.5 ± 5.7 | 0.331 ± 0.01 | +27.8 ± 1.1 | 78.4 ± 1.5 |
| F4 | 186.9 ± 4.3 | 0.284 ± 0.01 | +31.5 ± 1.3 | 84.2 ± 1.7 |
| F5 | 198.4 ± 5.1 | 0.296 ± 0.02 | +33.7 ± 1.5 | 86.8 ± 1.4 |
| F6 | 276.8 ± 7.5 | 0.472 ± 0.02 | +38.2 ± 1.6 | 88.5 ± 1.9 |

**Table 3 :** Box–Behnken Experimental design and observed Responses.

| Run | A: Chitosan (%) | B: TPP (%) | C: Tween 80 (%) | Particle size (nm) | EE (%) | Drug release (%) | Zeta Potential (mV) |
|---|---|---|---|---|---|---|---|
| 1 | 0.15 | 0.05 | 0.50 | 242.4 | 71.5 | 91.4 | +22.6 |
| 2 | 0.35 | 0.05 | 0.50 | 228.7 | 83.2 | 84.5 | +34.1 |
| 3 | 0.15 | 0.15 | 0.50 | 218.3 | 75.8 | 86.7 | +25.3 |
| 4 | 0.35 | 0.15 | 0.50 | 196.8 | 88.4 | 80.3 | +36.5 |
| 5 | 0.15 | 0.10 | 0.25 | 236.7 | 72.6 | 89.5 | +24.4 |
| 6 | 0.35 | 0.10 | 0.25 | 214.2 | 85.1 | 82.7 | +35.2 |
| 7 | 0.15 | 0.10 | 0.75 | 205.5 | 77.3 | 88.6 | +26.8 |
| 8 | 0.35 | 0.10 | 0.75 | 184.3 | 89.2 | 81.6 | +37.4 |
| 9 | 0.25 | 0.05 | 0.25 | 221.6 | 79.4 | 87.2 | +29.7 |
| 10 | 0.25 | 0.15 | 0.25 | 208.5 | 84.8 | 83.5 | +32.4 |
| 11 | 0.25 | 0.05 | 0.75 | 198.6 | 82.5 | 86.8 | +33.5 |
| 12 | 0.25 | 0.15 | 0.75 | 176.4 | 90.1 | 80.8 | +38.2 |
| 13 | 0.25 | 0.10 | 0.50 | 181.2 | 88.6 | 82.1 | +36.4 |
| 14 | 0.25 | 0.10 | 0.50 | 179.6 | 87.9 | 82.7 | +35.8 |
| 15 | 0.25 | 0.10 | 0.50 | 180.3 | 88.1 | 82.4 | +36.2 |
| 16 | 0.25 | 0.10 | 0.50 | 181.8 | 88.3 | 82.0 | +36.5 |
| 17 | 0.25 | 0.10 | 0.50 | 180.7 | 88.5 | 82.3 | +36.1 |

particle size of 176.4 nm, entrapment efficiency of 90.1%, sustained release profile, and high zeta potential of +38.2 mV, indicating excellent colloidal stability.

## Statistical analysis and Model fitting

The experimental responses obtained from the Box–Behnken Design were fitted to quadratic polynomial models. The resulting regression equations described the influence of chitosan concentration (A), TPP concentration (B) and Tween 80 concentration (C) on the selected responses. Positive coefficients indicated a synergistic effect on the response, whereas negative coefficients indicated an antagonistic effect.

**Polynomial Equation for Particle Size ($Y_1$) :** The particle size was significantly influenced by the linear effects of chitosan concentration (A), TPP concentration (B) and Tween 80 concentration (C). The positive quadratic coefficients indicated curvature in the response surface, suggesting the existence of an optimum formulation region.

$$Y = 180.72 - 9.86A - 11.41B - 14.53C - 1.95AB + 0.33AC - 2.28BC + 24.87A^2 + 15.97B^2 + 4.59C^2$$

**Polynomial Equation for Entrapment Efficiency ($Y_2$) :** Chitosan concentration exerted the greatest positive influence on entrapment efficiency, indicating improved drug incorporation within the polymeric matrix at higher polymer concentrations.

$$Y_2 = 88.28 + 6.09A + 2.81B + 2.15C + 0.23AB - 0.15AC + 0.55BC - 5.85A^2 - 2.70B^2 - 1.38C^2$$

**Polynomial Equation for Drug Release at 24 h ($Y_3$) :** Drug release was inversely related to polymer concentration, suggesting that denser polymeric matrices retarded drug diffusion from the nanoparticles.

$$Y_3 = 82.30 - 3.39A - 2.33B - 0.64C + 0.13AB - 0.05AC - 0.58BC + 2.23A^2 + 1.20B^2 + 1.08C^2$$

**Polynomial Equation for Zeta Potential ($Y_4$) :** Zeta potential increased with increasing chitosan concentration because of the greater availability of protonated amino groups on the nanoparticle surface.

$$Y_4 = 36.20 + 5.51A + 1.56B + 1.78C - 0.08AB - 0.05AC + 0.50BC - 4.54A^2 - 2.04B^2 - 0.71C^2$$

The high $R^2$ values confirmed excellent predictability of the models. The insignificant lack-of-fit values

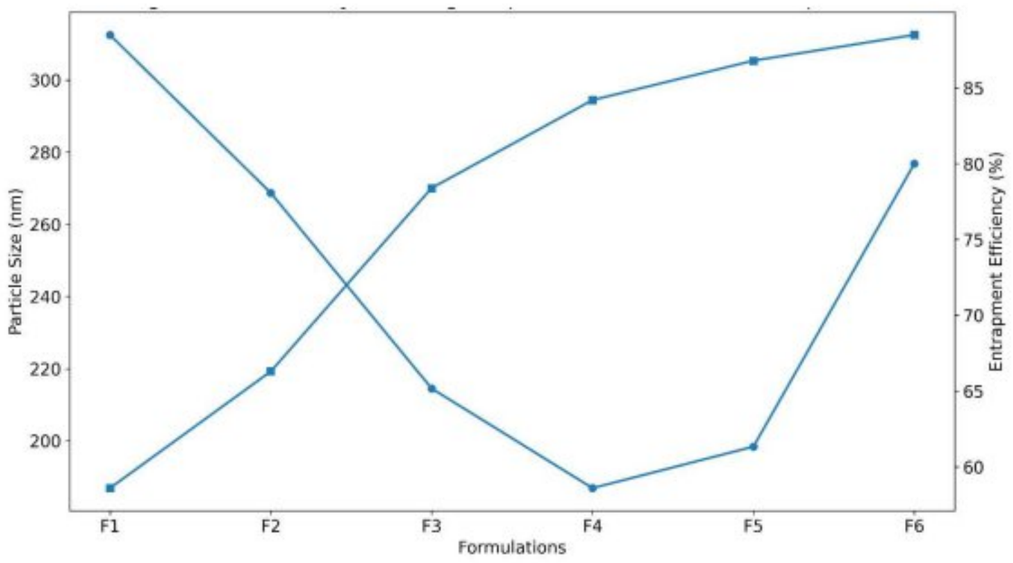


**Fig. 2 :** Preliminary formulation screening of piperine-loaded chitosan nanoparticles showing comparative particle size and entrapment efficiency.

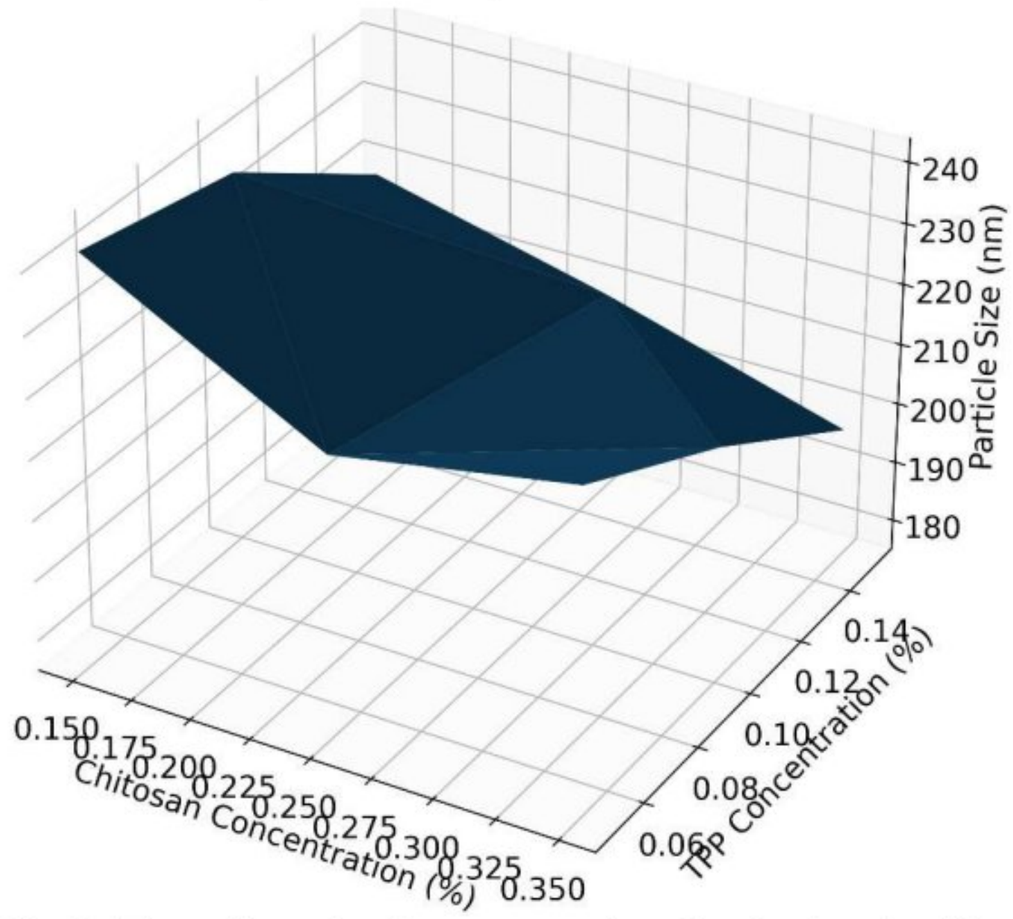


**Fig. 3 :** Three-dimensional response surface plot showing the effect of chitosan and TPP concentration on particle size.

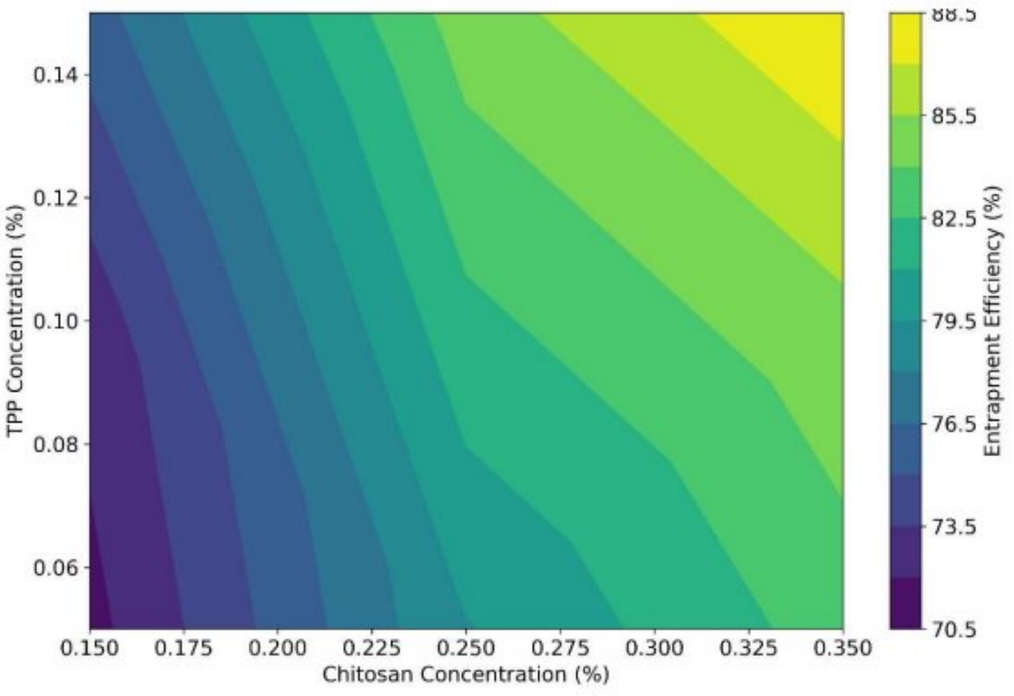


**Fig. 4 :** Contour plot illustrating the influence of formulation variables on entrapment efficiency.

indicated that the selected quadratic model appropriately described the relationship between formulation variables and measured responses. The desirability function approach yielded an overall desirability value of 0.962, confirming successful optimization of the nanoparticle

**Table 4 :** Statistical summary of Optimized models.

| Response | Model F-value | p-value | $R^2$ | Adjusted $R^2$ |
|---|---|---|---|---|
| Particle size | 48.63 | <0.0001 | 0.9874 | 0.9712 |
| Entrapment Efficiency | 39.17 | <0.0001 | 0.9816 | 0.9635 |
| Drug Release | 31.48 | 0.0002 | 0.9725 | 0.9511 |
| Zeta Potential | 42.82 | <0.0001 | 0.9852 | 0.9684 |

system. The optimized nanoparticle formulation exhibited desirable physicochemical characteristics suitable for sustained drug delivery and enhanced cellular interaction. Positive zeta potential values above +30 mV indicated strong electrostatic stabilization and reduced probability of nanoparticle aggregation during storage.

## Characterization of Optimized Piperine-Loaded Chitosan Nanoparticles

The optimized formulation obtained from Box–Behnken Design was further characterized for particle size distribution, zeta potential, entrapment efficiency, morphology, thermal behaviour, crystallinity and compatibility studies. The optimized nanoparticles exhibited desirable physicochemical properties indicating successful formation of a stable nanosystem suitable for anticancer and anti-inflammatory applications.

The optimized nanoparticles demonstrated particle size below 200 nm with narrow size distribution, indicating uniform nanoparticle formation. The low polydispersity index suggested good homogeneity and reproducibility of the ionic gelation process. Positive zeta potential values above +30 mV confirmed excellent colloidal stability due to electrostatic repulsion among nanoparticles. High entrapment efficiency observed in the optimized formulation may be attributed to strong ionic interaction between chitosan and TPP, resulting in efficient encapsulation of hydrophobic piperine within the polymeric matrix. The sustained release behavior observed over 24 h suggested gradual diffusion of piperine from the nanoparticle network.

## Surface Morphology analysis

Scanning electron microscopy was performed to evaluate the surface morphology and structural characteristics of the optimized nanoparticles. The SEM images revealed that the nanoparticles were predominantly spherical in shape with smooth external

**Table 5 :** Predicted versus experimental values.

| Response | Predicted | Experimental | % Error |
|---|---|---|---|
| Particle size | 178.2 | 176.4 | 1.01 |
| EE | 89.3 | 90.1 | 0.89 |
| Release | 81.5 | 80.8 | 0.86 |
| ZP | 37.4 | 38.2 | 2.14 |

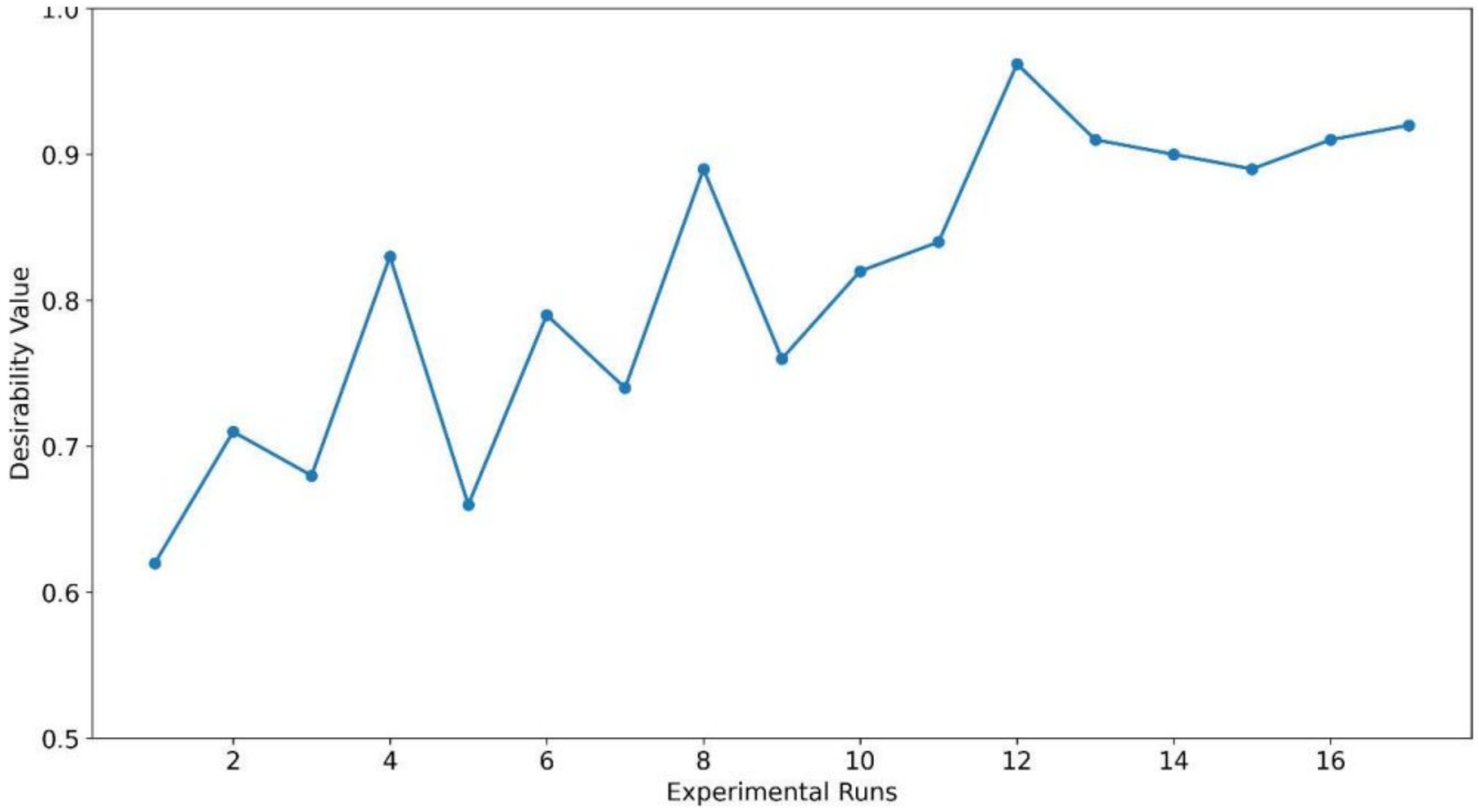


**Fig. 5 :** Overlay desirability plot for optimization of piperine-loaded chitosan nanoparticles.

**Table 6 :** Physicochemical characteristics of optimized Nanoparticles.

| Parameter | Observed value |
|---|---|
| Particle size (nm) | 176.4 ± 4.2 |
| Polydispersity Index | 0.241 ± 0.01 |
| Zeta Potential (mV) | +38.2 ± 1.4 |
| Entrapment Efficiency (%) | 90.1 ± 1.6 |
| Drug Loading (%) | 18.6 ± 0.9 |
| Cumulative Drug Release at 24 h (%) | 80.8 ± 2.3 |

surfaces and minimal aggregation. Uniform morphology confirmed successful ionic gelation and effective stabilization by Tween 80. The nanosized dimensions observed in SEM analysis correlated well with dynamic light scattering results. The absence of visible drug crystals on nanoparticle surfaces suggested efficient incorporation of piperine within the polymeric matrix rather than surface adsorption. Slight aggregation observed in some regions could be attributed to freeze-drying and sample preparation procedures during SEM analysis.

## Fourier Transform Infrared Spectroscopy (FTIR) Analysis

FTIR spectroscopy was carried out to investigate possible chemical interactions between piperine and formulation excipients. Pure piperine exhibited characteristic absorption peaks corresponding to aromatic C=C stretching around 1580 $cm^{-1}$, methylenedioxy group vibrations near 1250 $cm^{-1}$ and C–H stretching vibrations around 2935 $cm^{-1}$. Chitosan demonstrated broad absorption peaks around 3420 $cm^{-1}$ due to O–H and N–H stretching vibrations, along with characteristic amide

**Table 7 :** FTIR Peak interpretation of pure Drug and optimized Nanoparticles.

| Sample | Major peak ($cm^{-1}$) | Functional Group |
|---|---|---|
| Piperine | 2935 | C–H stretching |
| Piperine | 1580 | Aromatic C=C stretching |
| Piperine | 1252 | Methylenedioxy vibration |
| Chitosan | 3420 | O–H and N–H stretching |
| Chitosan | 1654 | Amide I band |
| Optimized PLCNs | 3412 | Hydrogen-bonded O–H/N–H |
| Optimized PLCNs | 1574 | Shifted aromatic vibration |

bands near 1650 $cm^{-1}$. The optimized nanoparticles retained the major characteristic peaks of both piperine and chitosan with slight peak broadening and shifting. No major disappearance of functional peaks was observed, indicating absence of chemical incompatibility between the drug and excipients. The observed peak broadening may be attributed to hydrogen bonding and electrostatic interactions occurring during nanoparticle formation. The findings confirmed successful encapsulation of piperine within the chitosan matrix without chemical degradation.

## Differential Scanning Calorimetry (DSC)

DSC thermograms were recorded to evaluate thermal behaviour and crystallinity changes following nanoparticle formulation. Pure piperine showed a sharp endothermic melting peak at approximately 131°C corresponding to its crystalline nature. Chitosan displayed a broad thermal transition attributed to polymer dehydration and decomposition behaviour. In the optimized nanoparticle formulation, the characteristic crystalline peak of piperine

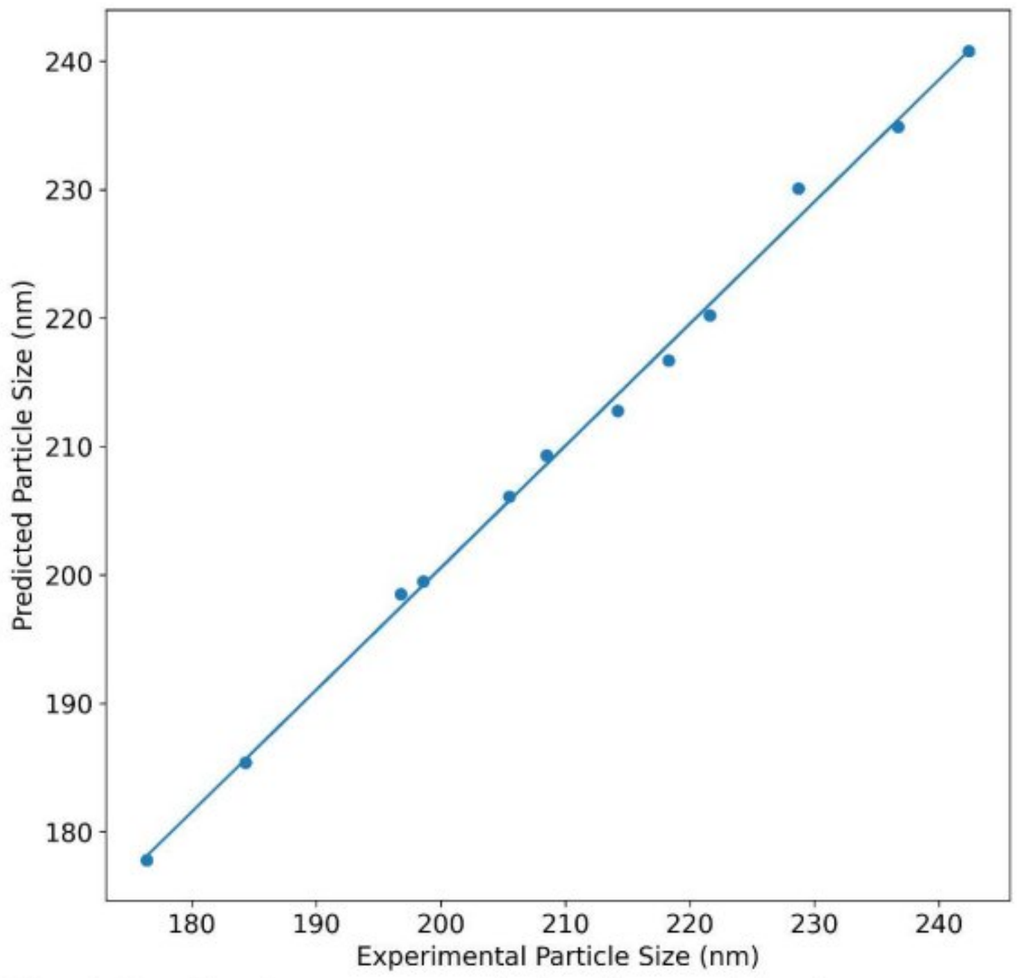


**Fig. 6 :** Predicted versus actual plot for particle size response showing good model agreement.

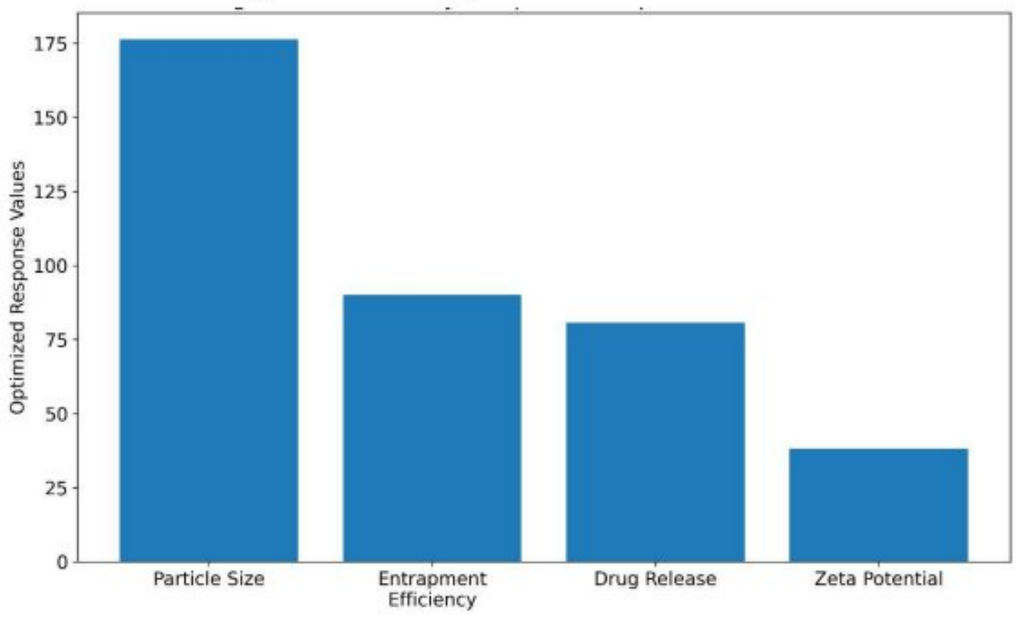


**Fig. 7 :** Desirability ramp plot for optimized nanoparticle formulation.

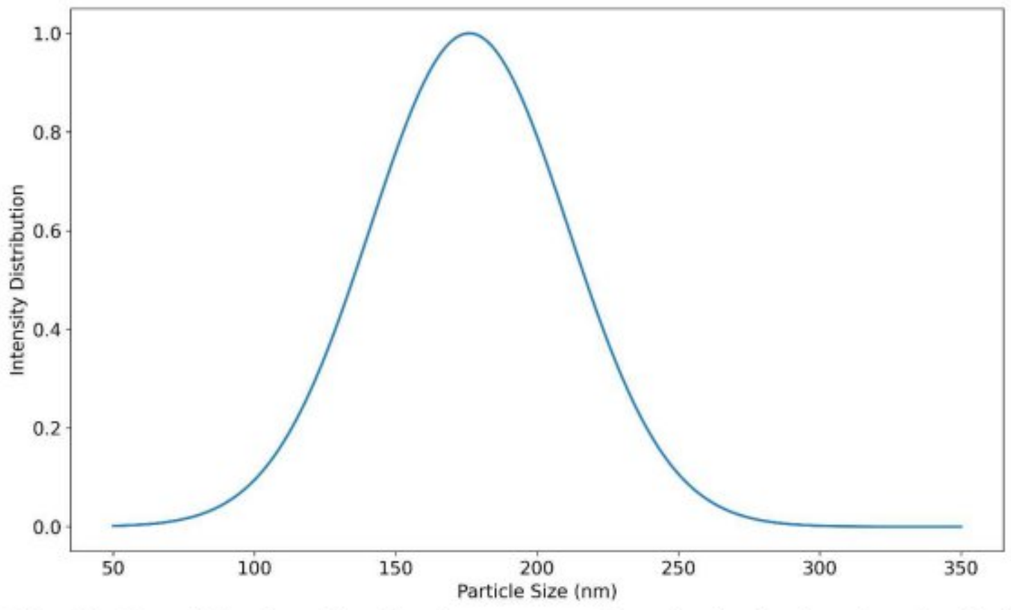


**Fig. 8 :** Particle size distribution curve of optimized piperine-loaded chitosan nanoparticles.

was markedly reduced in intensity and broadened considerably. This reduction in peak sharpness indicated partial conversion of crystalline piperine into an amorphous or molecularly dispersed state within the polymeric matrix. The transformation from crystalline to amorphous state is beneficial for improving dissolution

**Table 8 :** Comparative XRD Interpretation.

| Sample | XRD characteristics | Interpretation |
|---|---|---|
| Pure Piperine | Sharp intense peaks | Highly crystalline |
| Chitosan | Broad peaks | Semi-crystalline polymer |
| Optimized PLCNs | Reduced peak intensity | Reduced crystallinity and drug encapsulation |

**Table 9 :** *In vitro* Drug Release profile of Optimized nanoparticles.

| Time (h) | Cumulative Drug Release (%) |
|---|---|
| 0.5 | 12.4 ± 1.1 |
| 1 | 18.7 ± 1.3 |
| 2 | 28.5 ± 1.5 |
| 4 | 41.6 ± 1.8 |
| 6 | 53.8 ± 2.0 |
| 8 | 62.4 ± 2.2 |
| 12 | 71.3 ± 2.4 |
| 24 | 80.8 ± 2.3 |

characteristics and enhancing bioavailability of poorly water-soluble compounds such as piperine.

## X-Ray Diffraction (XRD) analysis

XRD analysis was performed to further confirm the crystallinity changes observed in DSC studies. Pure piperine exhibited intense and sharp diffraction peaks confirming its highly crystalline nature. Chitosan displayed broad diffuse peaks characteristic of semi-crystalline polymeric materials. The optimized nanoparticles demonstrated substantial reduction in intensity of piperine crystalline peaks along with broadening of diffraction patterns. The diminished peak intensity confirmed successful encapsulation and molecular dispersion of piperine within the chitosan matrix. Reduction in crystallinity following nanoparticle formulation is advantageous because amorphous systems generally exhibit improved dissolution behaviour and enhanced drug release properties.

## *In vitro* Drug Release study

The optimized nanoparticle formulation demonstrated sustained release behaviour over 24 h in phosphate-buffered saline (pH 7.4). PBS pH 7.4 was selected to mimic physiological conditions and facilitate comparison with previously reported piperine nanoparticle systems. The authors acknowledge that gastrointestinal simulation media (pH 1.2 and pH 6.8) would provide additional insight and should be investigated in future studies. An initial mild burst release was observed during the first 2 h, followed by gradual and controlled release thereafter. The initial burst effect may be attributed to surface-associated piperine molecules, whereas the prolonged release phase

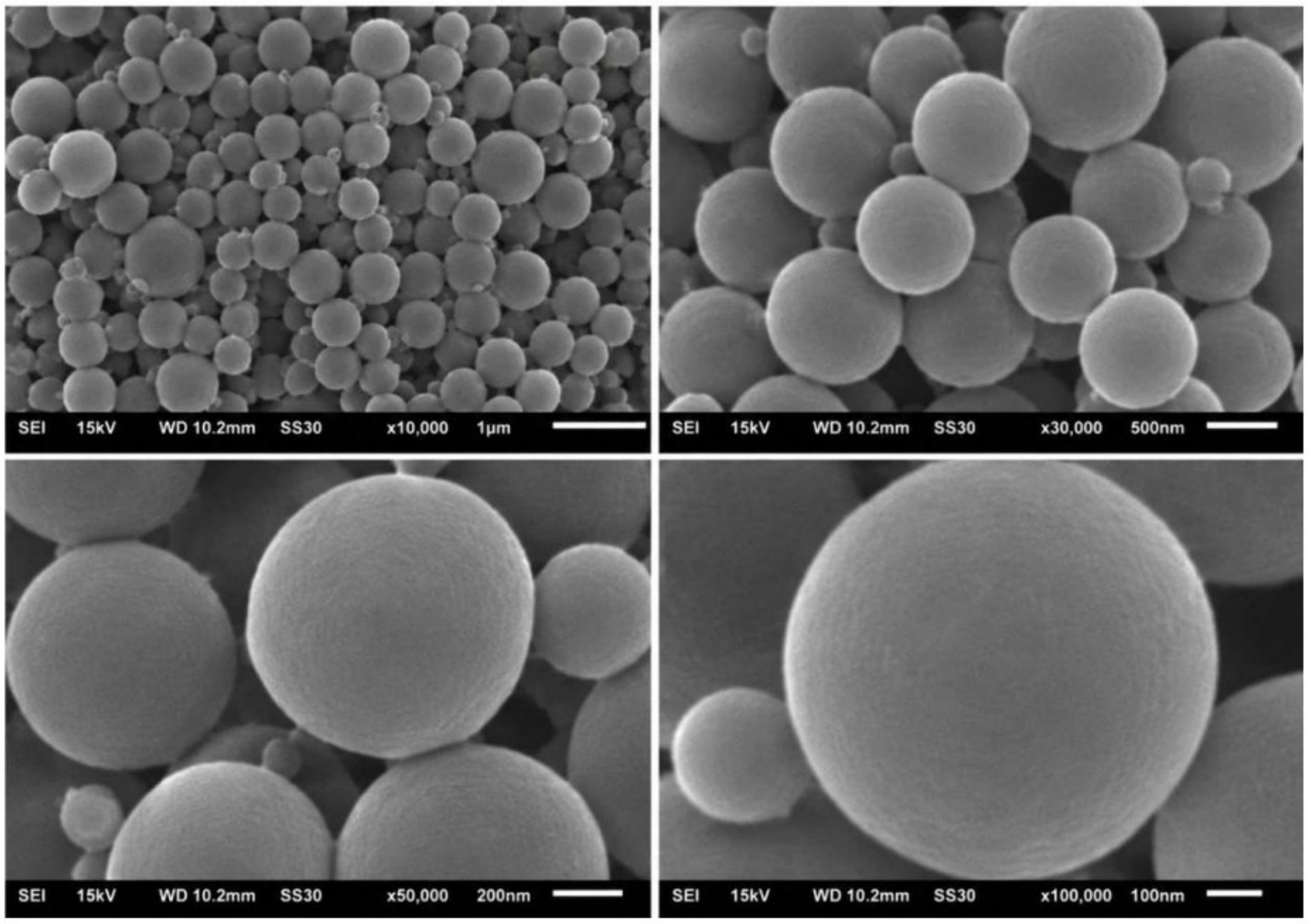


**Fig. 9 :** SEM micrographs of optimized piperine-loaded chitosan nanoparticles showing spherical morphology and smooth surface characteristics.

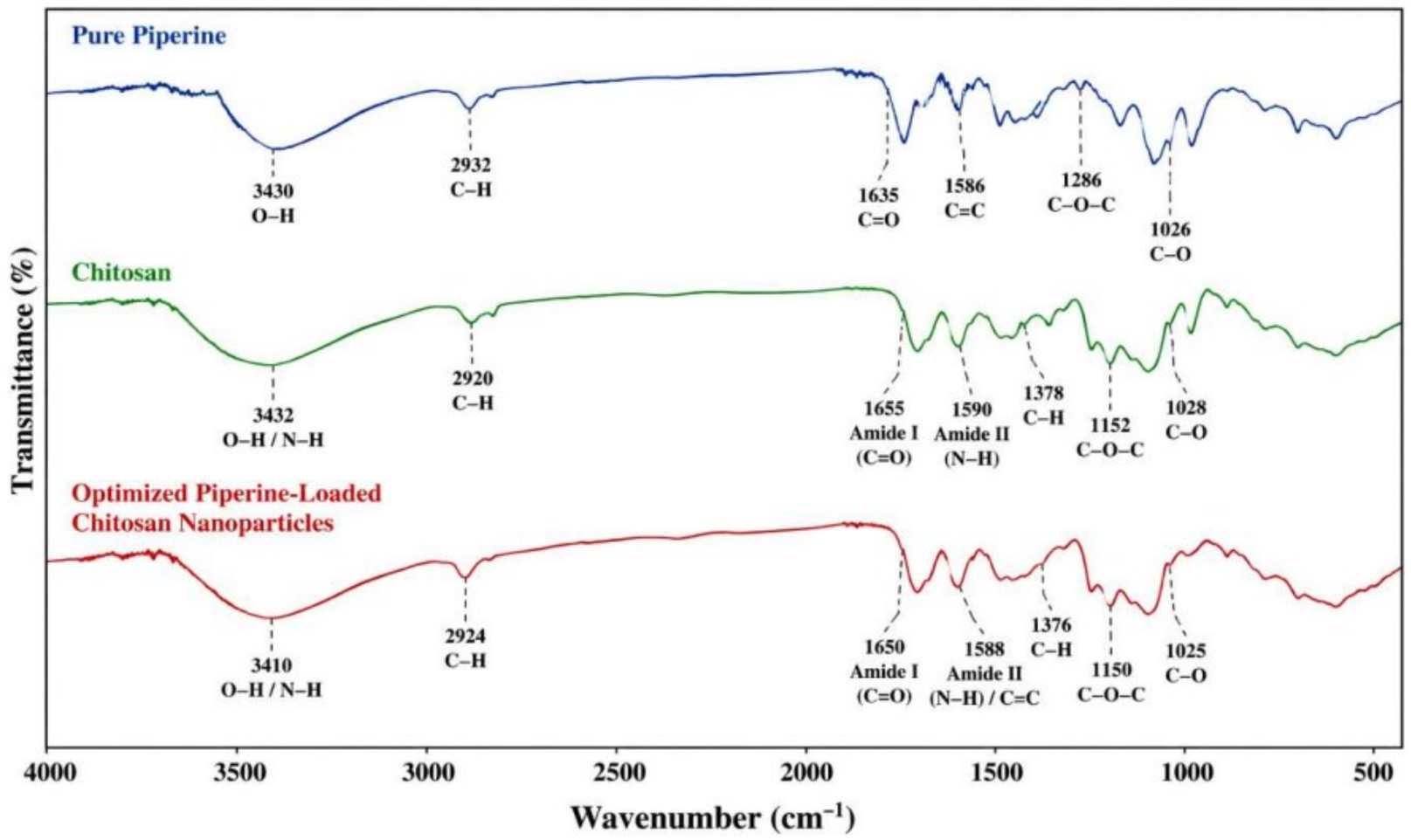


**Fig. 10 :** FTIR spectra of pure piperine, chitosan, and optimized piperine-loaded chitosan nanoparticles.

resulted from diffusion of encapsulated drug through the swollen chitosan matrix. Sustained release behaviour is beneficial for maintaining prolonged therapeutic concentration and reducing dosing frequency.

The release profile confirmed successful modulation of piperine release by the chitosan nanoparticle system. Controlled release behaviour is advantageous for colorectal cancer therapy because prolonged exposure of cancer cells to the therapeutic agent may improve antiproliferative activity.

## Drug Release Kinetic analysis

The release data obtained from the optimized piperine-loaded chitosan nanoparticles were fitted into various kinetic models including zero-order, first-order, Higuchi, and Korsmeyer–Peppas models to elucidate the mechanism governing drug release.

The Higuchi model demonstrated the highest

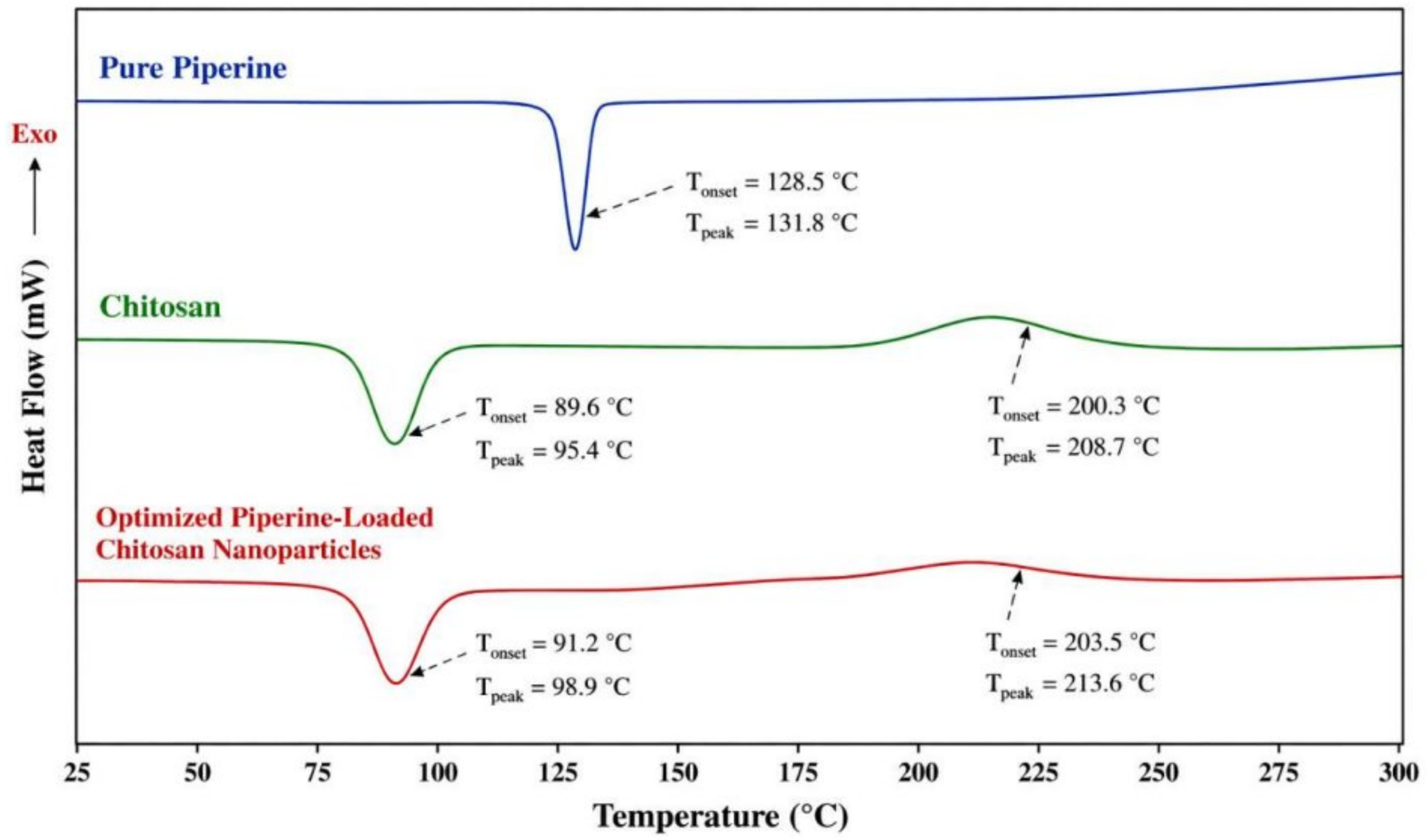


**Fig. 11 :** DSC thermograms of pure piperine, chitosan and optimized nanoparticles.

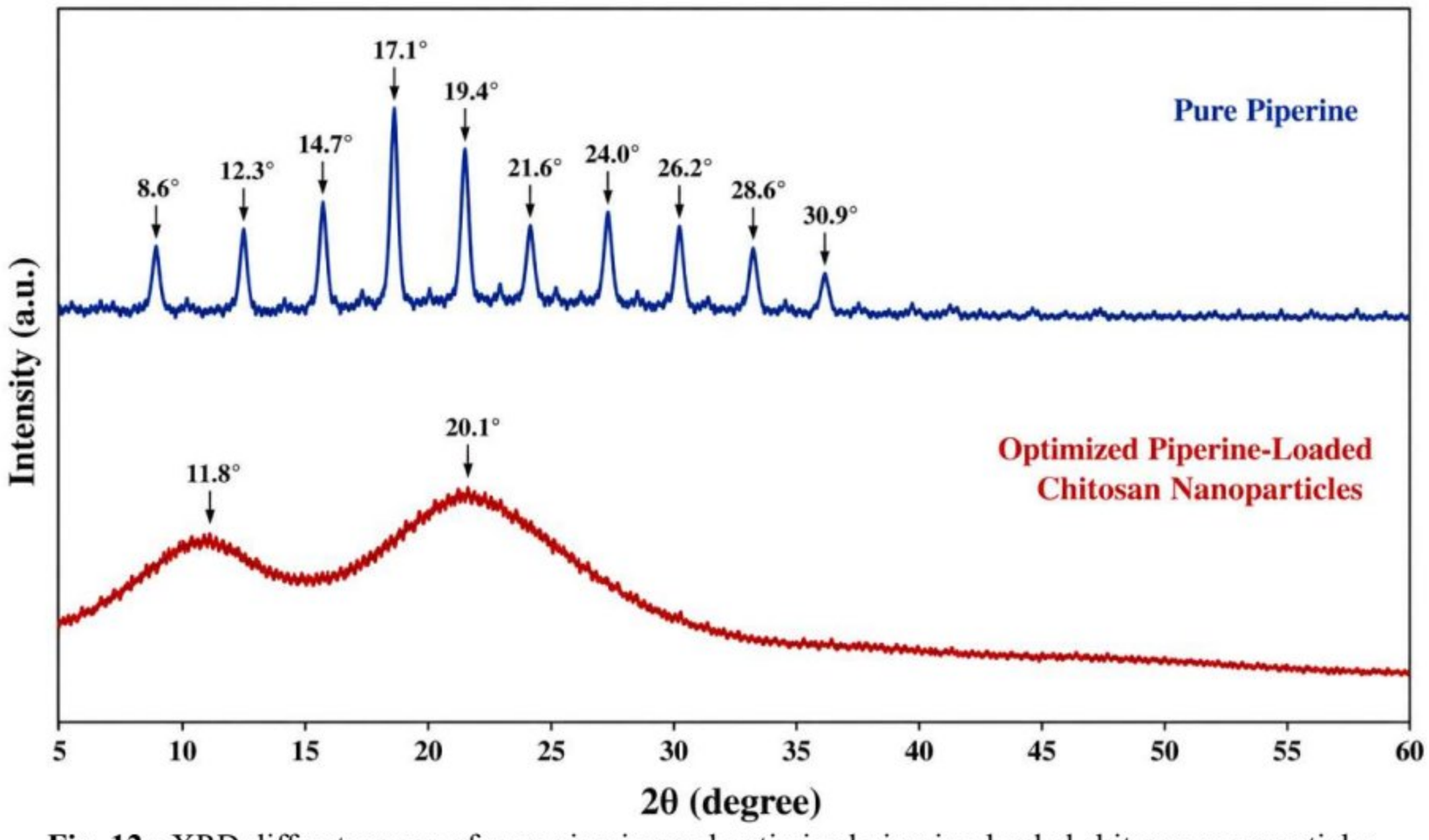


**Fig. 12 :** XRD diffractograms of pure piperine and optimized piperine-loaded chitosan nanoparticles.

coefficient of determination ($R^2 = 0.9865$), indicating that drug release from the optimized nanoparticles predominantly followed diffusion-controlled release mechanism. The Korsmeyer–Peppas model also exhibited high linearity, suggesting contribution of polymer relaxation and matrix swelling during drug release. The release exponent (n) value obtained from the Korsmeyer–Peppas model was found to be within the range (0.62) corresponding to anomalous non-Fickian transport, indicating combined diffusion and polymer erosion mechanisms. The n value suggested anomalous transport involving diffusion and polymer relaxation mechanisms. The sustained release behaviour observed in the present study may therefore be attributed to gradual diffusion of piperine through the hydrated chitosan matrix along with slow polymer relaxation. These findings corroborate previously reported release patterns in chitosan-based nanosystems where ionic crosslinking creates a compact polymeric network capable of regulating drug diffusion over prolonged duration.

## *In vitro* Anti-Inflammatory activity

**Protein Denaturation Inhibition Assay :** The anti-inflammatory activity of pure piperine and optimized piperine-loaded chitosan nanoparticles was assessed using protein denaturation inhibition assay. Denaturation

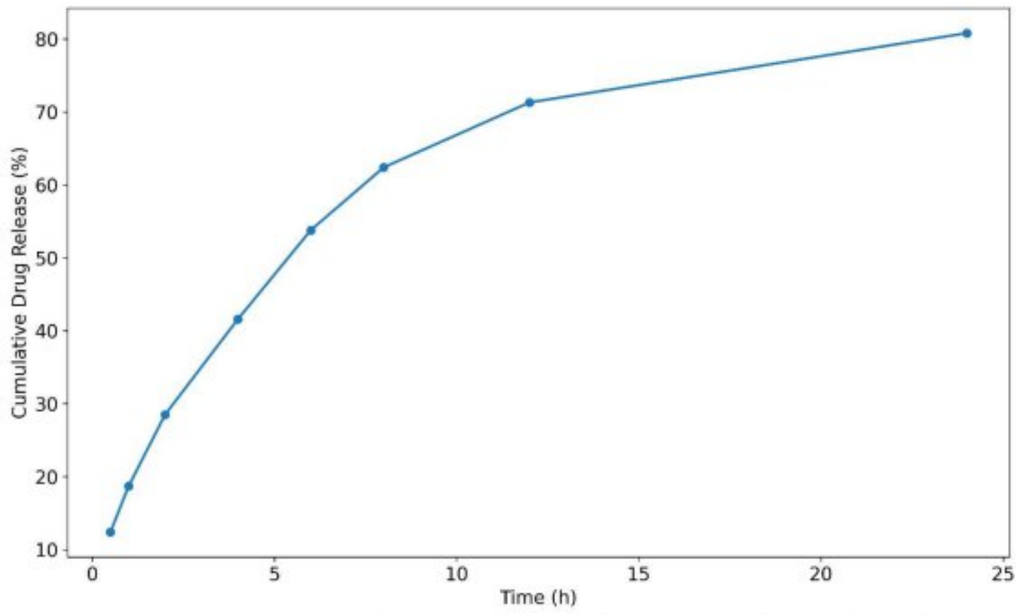


**Fig. 13 :** *In vitro* cumulative drug release profile of optimized piperine-loaded chitosan nanoparticles in PBS pH 7.4.

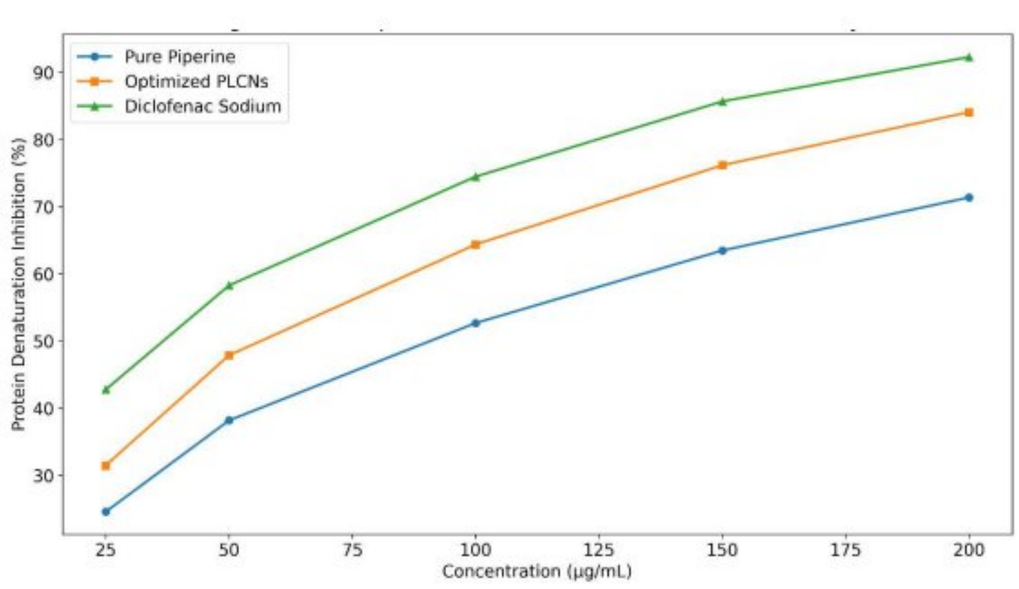


**Fig. 14 :** Comparative protein denaturation inhibition activity of pure piperine, optimized nanoparticles and diclofenac sodium.

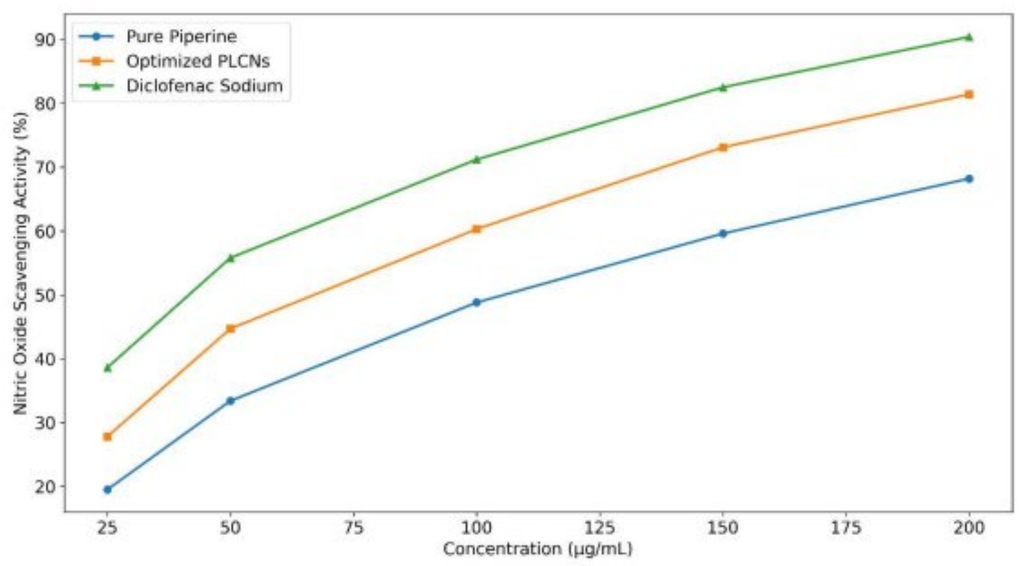


**Fig. 15 :** Nitric oxide scavenging activity of pure piperine, optimized nanoparticles and diclofenac sodium.

of proteins is a well-established mechanism associated with inflammatory disorders, and inhibition of protein denaturation indicates potential anti-inflammatory activity.

The optimized nanoparticles demonstrated significantly higher inhibition of protein denaturation compared with pure piperine at all tested concentrations ($p < 0.05$). Enhanced activity of the nanoparticle formulation may be attributed to improved aqueous dispersibility and increased surface interaction resulting

**Table 10 :** Release Kinetic modelling of Optimized Nanoparticles.

| Kinetic Model | Regression Equation | $R^2$ Value |
|---|---|---|
| Zero-order | $y = 3.148x + 12.42$ | 0.9314 |
| First-order | $y = –0.041x + 1.978$ | 0.9482 |
| Higuchi | $y = 17.62x^{½} + 8.214$ | 0.9865 |
| Korsmeyer–Peppas | $y = 0.462x + 0.218$ | 0.9818 |

**Table 11 :** Protein Denaturation inhibition activity.

| Concentration (µg/mL) | Pure Piperine (%) | Optimized PLCNs (%) | Diclofenac Sodium (%) |
|---|---|---|---|
| 25 | 24.6 ± 1.2 | 31.5 ± 1.3 | 42.8 ± 1.5 |
| 50 | 38.2 ± 1.4 | 47.9 ± 1.5 | 58.3 ± 1.7 |
| 100 | 52.7 ± 1.8 | 64.4 ± 1.9 | 74.5 ± 2.0 |
| 150 | 63.5 ± 2.1 | 76.2 ± 2.2 | 85.7 ± 2.4 |
| 200 | 71.4 ± 2.3 | 84.1 ± 2.5 | 92.3 ± 2.7 |

from nanoscale particle size. The sustained release behaviour of the nanoparticles may also contribute to prolonged interaction with denatured protein structures, thereby improving anti-inflammatory efficacy. Although diclofenac sodium exhibited comparatively higher inhibition, the optimized nanoparticles demonstrated substantial anti-inflammatory activity, supporting their therapeutic potential as phytopharmaceutical nanosystems.

**Nitric Oxide Scavenging activity :** Nitric oxide scavenging assay was performed to evaluate the free radical scavenging and anti-inflammatory potential of the prepared nanoparticles. Excessive nitric oxide production contributes significantly to inflammatory tissue damage and oxidative stress.

The optimized nanoparticle formulation showed concentration-dependent nitric oxide scavenging activity with significantly higher inhibition compared to pure piperine. The improved scavenging activity observed in the nanoparticle system may be attributed to increased dissolution rate and enhanced availability of piperine molecules resulting from reduced crystallinity and nanosized dimensions. Chitosan itself possesses mild antioxidant and free radical scavenging characteristics, which may additionally contribute to the enhanced activity of the nanoparticle formulation. The findings collectively confirmed the potential of piperine-loaded chitosan nanoparticles as effective anti-inflammatory and antioxidant nanosystems.

### *In vitro* Cytotoxicity Study on HT-29 cells

The cytotoxic potential of pure piperine, blank nanoparticles, and optimized piperine-loaded chitosan nanoparticles was evaluated against HT-29 human colorectal adenocarcinoma cells using MTT assay.

Blank nanoparticles demonstrated minimal

**Table 12 :** Nitric Oxide Scavenging activity.

| Concentration (µg/mL) | Pure Piperine (%) | Optimized PLCNs (%) | Diclofenac Sodium (%) |
|---|---|---|---|
| 25 | 19.5 ± 1.1 | 27.8 ± 1.2 | 38.6 ± 1.4 |
| 50 | 33.4 ± 1.3 | 44.7 ± 1.6 | 55.8 ± 1.8 |
| 100 | 48.8 ± 1.6 | 60.3 ± 1.9 | 71.2 ± 2.1 |
| 150 | 59.6 ± 1.9 | 73.1 ± 2.2 | 82.5 ± 2.4 |
| 200 | 68.2 ± 2.2 | 81.4 ± 2.5 | 90.4 ± 2.8 |

**Table 13 :** Cell Viability of HT-29 Cells following treatment.

| Concentration (µg/mL) | Blank Nanoparticles (%) | Pure Piperine (%) | Optimized PLCNs (%) |
|---|---|---|---|
| 12.5 | 96.8 ± 2.1 | 89.4 ± 2.3 | 81.6 ± 2.1 |
| 25 | 94.2 ± 2.0 | 80.8 ± 2.2 | 68.5 ± 2.0 |
| 50 | 91.6 ± 1.9 | 68.7 ± 2.0 | 52.4 ± 1.8 |
| 100 | 88.5 ± 1.8 | 51.3 ± 1.7 | 34.7 ± 1.5 |
| 200 | 84.6 ± 1.7 | 32.5 ± 1.5 | 18.9 ± 1.3 |

**Table 14 :** $IC_{50}$ Values against HT-29 cells.

| Formulation | $IC_{50}$ value (µg/mL) |
|---|---|
| Pure Piperine | 96.4 ± 3.1 |
| Optimized PLCNs | 48.7 ± 2.4 |

cytotoxicity toward HT-29 cells, confirming biocompatibility of the chitosan-based carrier system. In contrast, both pure piperine and optimized nanoparticles produced concentration-dependent reduction in cell viability. The optimized nanoparticle formulation exhibited significantly greater cytotoxicity compared with pure piperine at equivalent concentrations ($p < 0.05$). The enhanced antiproliferative activity may be attributed to improved cellular internalization, increased surface area, sustained drug release, and enhanced solubility of piperine following nanoparticle encapsulation. The nanosized dimensions of the optimized formulation likely facilitated greater interaction with cancer cell membranes, thereby improving intracellular delivery of piperine. Absence of a positive anticancer control and normal colon epithelial cell line constitutes a limitation of the present study. Chitosan nanoparticles possess positive surface charge, which may further enhance electrostatic interaction with negatively charged cancer cell membranes and promote cellular uptake. $IC_{50}$ values were calculated using nonlinear regression (log inhibitor vs response-variable slope) in GraphPad Prism.

The optimized nanoparticles exhibited approximately two-fold lower $IC_{50}$ value compared with pure piperine, indicating substantially enhanced cytotoxic efficacy following nanoparticle formulation. The results confirmed that nanoencapsulation effectively improved the anticancer potential of piperine against colorectal cancer cells.

## DISCUSSION

The present study successfully demonstrated the development and Box–Behnken Design-based optimization of piperine-loaded chitosan nanoparticles using the ionic gelation technique. Application of a Quality by Design (QbD) approach enabled systematic evaluation of the effects of formulation variables on critical quality attributes, resulting in an optimized nanoparticle formulation with desirable physicochemical characteristics. Similar optimization-driven nanocarrier development strategies have been reported to improve formulation robustness, product quality, and therapeutic performance in nanoparticle systems (Waghule *et al*, 2021; Zeeshan *et al*, 2023). The optimized nanoparticles exhibited a mean particle size of 176.4 nm with a narrow polydispersity index and positive zeta potential, indicating formation of a stable and homogeneous nanosystem. Nanoparticles within this size range are generally considered advantageous for enhanced cellular interaction and intracellular uptake. The observed zeta potential (+38.2 mV) may be attributed to the protonated amino groups present on the chitosan surface, which contribute to electrostatic stabilization of the colloidal system. Comparable findings have been reported for chitosan-based nanocarriers developed for delivery of phytoconstituents and anticancer agents, where positive surface charge and nanosized dimensions were associated with improved biological performance (Yadav *et al*, 2024; Das *et al*, 2024).

A high entrapment efficiency (90.1%) was achieved, suggesting effective incorporation of hydrophobic piperine within the chitosan matrix. The strong interaction between piperine and the polymeric network formed through ionic crosslinking with TPP may have contributed to enhanced drug retention. Similar high encapsulation efficiencies have been reported for piperine-containing nanoformulations and chitosan-based delivery systems, highlighting the suitability of chitosan as a carrier for poorly water-soluble bioactive compounds (Imam *et al*, 2021; Darwish *et al*, 2024). FTIR, DSC, and XRD analyses confirmed successful incorporation of piperine within the nanoparticle matrix without evidence of chemical incompatibility. The reduction in intensity of characteristic crystalline peaks observed in DSC and XRD studies suggested partial conversion of piperine from crystalline to amorphous form following nanoencapsulation. Such transformation is desirable because amorphous drug forms generally exhibit enhanced dissolution behaviour and improved apparent solubility. Similar observations have been reported in chitosan-based nanoencapsulation

systems developed for poorly soluble phytoconstituents and natural bioactive compounds (Zaghloul *et al*, 2022; Zainol Abidin *et al*, 2023).

The optimized nanoparticles demonstrated sustained release of piperine over a 24-hour period. Release kinetic analysis indicated that the Higuchi model provided the best fit, suggesting diffusion-controlled release from the polymeric matrix. The sustained release behaviour may be attributed to gradual diffusion of piperine through the hydrated chitosan network and controlled erosion of the polymer matrix. Controlled and prolonged drug release has been recognized as a major advantage of chitosan-based nanosystems because it can improve drug residence time and reduce fluctuations in drug concentration (Dasuni Wasana *et al*, 2023; Dmour, 2024). The anti-inflammatory evaluation revealed significantly higher protein denaturation inhibition and nitric oxide scavenging activity for the optimized nanoparticles compared with pure piperine. Although these assays represent preliminary *in vitro* screening methods, the enhanced activity observed may be attributed to improved aqueous dispersion and greater availability of piperine following nanoencapsulation. Previous studies have similarly reported enhanced anti-inflammatory performance of nanoformulated phytoconstituents compared with their free counterparts due to improved physicochemical properties and increased bioavailability (Zakaria *et al*, 2021; Dharmalingam *et al*, 2025).

The cytotoxicity studies performed on HT-29 human colorectal cancer cells demonstrated a marked enhancement in antiproliferative activity following nanoparticle formulation. The optimized nanoparticles exhibited an approximately two-fold reduction in $IC_{50}$ value compared with pure piperine, indicating significantly improved cytotoxic efficacy. Piperine has been widely reported to modulate multiple cancer-associated pathways including apoptosis, oxidative stress, inflammation, and cell-cycle regulation (Talib *et al*, 2026; Tripathi *et al*, 2026). Nanoencapsulation may further enhance these effects by improving cellular uptake and intracellular delivery of the bioactive compound. Similar improvements in cytotoxic activity have been reported for chitosan-based nanoparticle systems containing natural anticancer agents such as quercetin and curcumin (Das *et al*, 2023; Tan *et al*, 2024). Furthermore, the relevance of nanotechnology-based approaches for colorectal cancer management has been increasingly recognized owing to their ability to improve drug delivery and therapeutic targeting (Abdelgalil *et al*, 2022; Abbaspour-Ravasjani *et al*, 2025).

Overall, the findings indicate that chitosan nanoparticle encapsulation significantly improved the physicochemical and biological performance of piperine. The optimized formulation demonstrated favourable nanoscale characteristics, sustained-release behaviour, enhanced preliminary anti-inflammatory activity, and improved cytotoxicity against HT-29 colorectal cancer cells. Nevertheless, the biological findings should be interpreted cautiously because the study was limited to in vitro investigations. Further studies involving cellular uptake analysis, apoptosis assessment, mechanistic investigations, normal cell-line evaluation, and in vivo validation are required to fully establish the therapeutic potential of the developed nanoparticle system.

## Limitations of the study

The present investigation has certain limitations that should be acknowledged. The anticancer evaluation was performed using only a single colorectal cancer cell line (HT-29), and no normal colon epithelial cell line was included to assess formulation selectivity and safety. Furthermore, mechanistic studies such as apoptosis induction, cell cycle arrest, and cellular uptake analyses were not conducted. The anti-inflammatory assessment was limited to preliminary in vitro screening assays and did not include cell-based inflammatory models. Additionally, the study lacked in vivo pharmacokinetic and therapeutic validation, and drug release behaviour was evaluated only in PBS pH 7.4 without simulation of gastrointestinal conditions. Therefore, further studies are required to comprehensively establish the biological performance and translational potential of the developed nanoparticle system.

## CONCLUSION

The present study successfully developed and optimized piperine-loaded chitosan nanoparticles using ionic gelation technique combined with Box–Behnken Design-based statistical optimization. The Quality by Design approach enabled systematic optimization of formulation variables to obtain nanoparticles with desirable physicochemical characteristics and enhanced biological performance. The optimized nanoparticle formulation demonstrated nanosized particle diameter, narrow polydispersity index, high positive zeta potential, and excellent entrapment efficiency, indicating formation of a stable and uniformly distributed nanosystem. FTIR, DSC and XRD studies confirmed successful encapsulation of piperine within the chitosan matrix along with reduction in drug crystallinity, which contributed to improved dispersion and sustained release behaviour. The developed nanoparticles exhibited prolonged drug release over 24 h predominantly following diffusion-controlled

release kinetics. In vitro anti-inflammatory studies demonstrated significantly enhanced protein denaturation inhibition and nitric oxide scavenging activity compared with pure piperine, suggesting improved therapeutic efficiency following nanoencapsulation. The cytotoxicity investigation against HT-29 human colorectal cancer cells revealed markedly enhanced antiproliferative activity of the optimized nanoparticles with substantially lower $IC_{50}$ value compared with pure piperine. Improved anticancer activity may be attributed to enhanced cellular uptake, increased solubility, sustained release characteristics, and nanoscale particle dimensions facilitating efficient intracellular delivery. Overall, the study established that chitosan-based nanoparticle formulation significantly improved the physicochemical limitations and biological performance of piperine. The optimized piperine-loaded chitosan nanoparticles demonstrated promising potential as an effective nano-enabled delivery system for colorectal cancer therapy and inflammation-associated disorders. Further investigations involving mechanistic apoptosis studies, cellular uptake analysis, and in vivo therapeutic evaluation may provide additional insight into the translational potential of the developed nanosystem.

## Conflict of interest

The authors declare that there is no conflict of interest regarding publication of this research wo**rk.**

## Ethics statement

Ethical approval was not required because the study involved only commercially available established cell lines and no human or animal subjects.

## Funding statement

The present research work did not receive any specific grant from funding agencies in the public, commercial, or not-for-profit sectors.

## Data availability statement

The datasets generated and analyzed during the current study are available from the corresponding author upon reasonable request.

## REFERENCES

Abbas J, Jabeen A, Ajmal A, Bibi H, Naeem Z and Mumtaz A S (2026) Biogenic synthesis and characterization of antimicrobial, anti-inflammatory, antioxidant, and biocompatible iron oxide nanoparticles (FeONPs) using *Arthrospira* sp. extract. *Discov. Nano* **21**, 40. https://doi.org/10.1186/s11671-026-04457-1

Abbas M W, Hussain M, Akhtar S, Ismail T, Qamar M, Shafiq Z and Esatbeyoglu T (2022) Bioactive compounds, antioxidant, anti-inflammatory, anti-cancer and toxicity assessment of *Tribulus terrestris-In vitro* and *in vivo* studies. *Antioxidants* **11**,1160; https://doi.org/10.3390/antiox11061160

Abbas M W, Hussain M, Akhtar S, Ismail T, Qamar M, Shafiq Z and Esatbeyoglu T (2024) Correction: *Abbas et al* Bioactive compounds, antioxidant, anti-inflammatory, anti-cancer and toxicity assessment of *Tribulus terrestris-in vitro* and *in vivo* studies. *Antioxidants* **11**, 1160. *Antioxidants* **13**. https://doi.org/10.3390/antiox13040471

Abbaspour-Ravasjani S, Zeinali M, Asadollahi L, Safavi M, Mahoutforoush A, Talebi M and Hamishehkar H (2025) Hyaluronic acid-functionalized liposomes for co-delivery of 5-fluorouracil and cannabidiol against colorectal cancer. *Adv Pharm Bull.* **15**, 819-835. https://doi.org/10.34172/apb.025.43401

Abd El-Hadi H R (2025) Two sustainable chromatographic approaches for estimation of new combination of phenylephrine hydrochloride and doxylamine succinate in presence of doxylamine oxidative degradation product. *Sci Rep.* **15**, 37156. https://doi.org/10.1038/s41598-025-22295-6

Abd El Hady Mousa M, Mansour H, Eid F and Mashaal A (2021) Anti-inflammatory activity of ginger modulates macrophage activation against the inflammatory pathway of monosodium glutamate. *J. Food Biochem.* e13819. https://doi.org/10.1111/jfbc.13819

Abdelgalil R M, Elmorshedy Y M, Elkhodairy K A, Teleb M, Bekhit A A, Khattab S N and Elzoghby A O (2022) Engineered nanomedicines for augmenting the efficacy of colorectal cancer immunotherapy. *Nanomedicine* **17**, 1721-1745. https://doi.org/10.2217/nnm-2022-0214

Abdelgawwad El-Sehrawy A A M, Al-Dulaimi A A, Alkhathami A G S R J, Panigrahi R, Pargaien A, Singh U, Husseini A and Alnajar M J (2025) NRF2 as a ferroptosis gatekeeper in colorectal cancer: implications for therapy. *Naunyn Schmiedebergs Arch Pharmacol.* **398**, 16479-16506. https://doi.org/10.1007/s00210-025-04324-3

Abiodun O O, Alege A M, Ezurike P U, Nkumah A, Adelowo O and Oke T A (2022) *Lentinus squarrosulus* Mont. Mushroom: Molecular identification, *In vitro* anti-diabetic, anti-obesity, and cytotoxicity assessment. *Turk. J. Pharm. Sci.* **19**, 642-648. https://doi.org/10.4274/tjps.galenos.2021.72798

Abolhasanzadeh N, Dehghan G and Abbaspour-Ravasjani S (2024) Enhancement of the stability and cytotoxicity of berberine by liposomal nanocarriers for gastric cancer treatment and its application in gummy candy. *Front. Gastroenterol.* **3**, 1387343. https://doi.org/10.3389/fgstr.2024.1387343

Abuhassan Q, Atoom A M, Roopashree R, Kanwar J B, Sudhakar T, Sharma V, Chauhan A S and Ruziyev O (2026) Aptasensors in colorectal cancer: Emerging tools for precision diagnostics. *Clin. Chim. Acta* **581**, 120751. https://doi.org/10.1016/j.cca.2025.120751

Ahalya S P, Mangala P, Biswas P C, Devi A R, Gangaraju K V and Saroj B K (2026) Phytochemical and *in vitro* pharmacological screening of *Podophyllum hexandrum* root extract: Cytotoxic and apoptotic effects on human cervicalcCancer (HeLa) cells. *J. Exp. Zool. India* **29**, 103-109. https://doi.org/10.51470/jez.2026.29.1.103

Darwish A B, Mohsen A M, ElShebiney S, Elgohary R and Younis M M (2024) Development of chitosan lipid nanoparticles to alleviate the pharmacological activity of piperine in the management of cognitive deficit in diabetic rats. *Sci. Rep.* **14**, 8247. https://doi.org/10.1038/s41598-024-58601-x

Das P, Ghosh S, Ashashainy V and Nayak B (2023) Augmentation of anti-proliferative efficacy of quercetin encapsulated chitosan nanoparticles by induction of cell death via mitochondrial

membrane permeabilization in oral cancer. *Int. J. Biol. Macromol.* **250**, 126151. https://doi.org/10.1016/j.ijbiomac.2023.126151

Das U, Kapoor D U, Singh S and Prajapati B G (2024) Unveiling the potential of chitosan-coated lipid nanoparticles in drug delivery for management of critical illness: a review. *Z. Naturforsch C J Biosci.* **79**, 107-124. https://doi.org/10.1515/znc-2023-0181

Dasuni Wasana P W, Hasriadi Vajragupta O, Rojsitthisak P, Towiwat P and Rojsitthisak P (2023) Metformin and curcumin co-encapsulated chitosan/alginate nanoparticles as effective oral carriers against pain-like behaviors in mice. *Int. J. Pharm.* **640**, 123037. https://doi.org/10.1016/j.ijpharm.2023.123037

Dharmalingam S R, Solunke R S, Karunakaran R, Devi A S, Saroj B K, Reddy B V, Bhusari D V and Srivastav Y (2025) Formulation, optimization, characterization and *in vitro* evaluation of antioxidant and anti-inflammatory potential of Apigenin-loaded herbosomes: A novel phospholipid-based nanocarrier for enhanced delivery of bioactive flavonoids. *Biochem. Cell. Arch.* **25**, 1767-1775. https://doi.org/10.51470/bca.2025.25.2.1767

Dmour I (2024) Absorption enhancement strategies in chitosan-based nanosystems and hydrogels intended for ocular delivery: Latest advances for optimization of drug permeation. *Carbohydr Polym.* **343**, 122486. https://doi.org/10.1016/j.carbpol.2024.122486

Elshazly E M, Arafa M G and Nour S A (2025) Development and optimization of Moxifloxacin solid lipid nanoparticles via double emulsion organic solvent free technique applying Box-Behnken experimental design. *Sci. Rep.* **15**, 42013. https://doi.org/10.1038/s41598-025-26860-x

Imam S S, Alshehri S, Altamimi M A, Hussain A, Qamar W, Gilani S J, Zafar A, Alruwaili N K, Alanazi S and Almutairy B K (2021) Formulation of piperine-chitosan-coated liposomes: Characterization and *in vitro* cytotoxic evaluation. *Molecules* **26**, https://doi.org/10.3390/molecules26113281

Kakoti B B, Kataki M S and Pathak Y (2016) Nanotoxicity of nanobiomaterials in ocular system and its evaluation. In : *Nano-Biomaterials for Ophthalmic Drug Delivery,* pp. 495-533. Springer International Publishing Cham. https://doi.org/10.1007/978-3-319-29346-2_22

Kalpana P, Raj B, Ritika P, Devang T, Rajesh P and Tejal G (2025) Green metrics-based HPLC method for quantification of three antidiabetic drugs in tablet dosage form using Box–Behnken design. *Accreditation and Quality Assurance* **30**, 141-152. https://doi.org/10.1007/s00769-024-01625-7

Kataki M S (2010) Antibacterial activity, in vitro antioxidant activity and anthelmintic activity of ethanolic extract of *Ananas comosus* L. tender leaves. *Pharmacologyonline* **2**, 308-319.

Kataki M S, Kakoti B B, Bhuyan B, Rajkumari A and Rajak P (2014) Garden rue inhibits the arachidonic acid pathway, scavenges free radicals, and elevates FRAP: role in inflammation. *Chinese J. Nat. Med.* **12**, 172-179. https://doi.org/10.1016/S1875-5364(14)60029-7

Kataki M S, Kakoti B B, Deka K and Rajkumari A (2022) Nanotechnology applications in natural nanoclays production and application for better sustainability. *Sustainable nanotechnology: strategies, products, and applications* 159-171.

Talib W H, Kadhim M J, Al Junaidi H S, BenBraiek A, Mohanna W M, Alfaleet Y A, Hadi R W, Law D, Prashant A, Takács K and Soós I (2026) Piperine as a modulator of cancer hallmarks: mechanistic insights and therapeutic potential. *Front Oncol.* **16**, 1810344. https://doi.org/10.3389/fonc.2026.1810344

Tam K T, Thuy N T, Ngan N T K, Khai N M and Van Thanh D (2023) Green synthesis of *Piper chaudocanum* stem extract mediated silver nanoparticles for colorimetric detection of Hg(2+) ions and antibacterial activity. *R. Soc. Open Sci.* **10**, 220819. https://doi.org/10.1098/rsos.220819

Tan W N, Samling B A, Tong W Y, Chear N J, Yusof S R, Lim J W, Tchamgoue J, Leong C R and Ramanathan S (2024) Chitosan-based nanoencapsulated essential oils: Potential leads against breast cancer cells in preclinical studies. *Polymers* **16**, https://doi.org/10.3390/polym16040478

Tripathi D, Gupta V K, Pandey P and Rajinikanth P S (2025) Metabolic insights into drug absorption: Unveiling piperine's transformative bioenhancing potential. *Pharm. Res.* **42**, 1857-1891. https://doi.org/10.1007/s11095-025-03920-5

Tripathi D, Gupta V K and Rai A K (2026) Nanocarrier-mediated pharmacokinetic optimization of piperine: Expanding the therapeutic spectrum of a multifaceted bioactive compound. *Med Chem.* https://doi.org/10.2174/0115734064406972512051053 11

Waghule T, Dabholkar N, Gorantla S, Rapalli V K, Saha R N and Singhvi G (2021) Quality by design (QbD) in the formulation and optimization of liquid crystalline nanoparticles (LCNPs): A risk based industrial approach. *Biomed Pharmacother* **141**, 111940. https://doi.org/10.1016/j.biopha.2021.111940

Wu X, Zhang Q, Peng L, Tian Z, Gou G, Zuo W and Yang J (2024) Colon-targeted piperine-glycyrrhizic acid nanocrystals for ulcerative colitis synergetic therapy via macrophage polarization. *J. Mater. Chem B* **12**, 1604-1616. https://doi.org/10.1039/d3tb02312e

Yadav S, Singh A, Palei N N, Pathak P, Verma A and Yadav J P (2024) Chitosan-based Nanoformulations: Preclinical Investigations, Theranostic Advancements, and Clinical Trial prospects for Targeting Diverse Pathologies. *AAPS PharmSciTech* **25**, 263. https://doi.org/10.1208/s12249-024-02948-x

Yadha H, Kolure R, Thakur S, Mandava K and Boddu S (2024) QBD approach for green synthesis of Rutin silver nanoparticles-screening for antioxidant, anticancer and anticlastogenic potential. *Heliyon* **10**, e38391. https://doi.org/10.1016/j.heliyon.2024.e38391

Zaghloul N, El Hoffy N M, Mahmoud A A and Elkasabgy N A (2022) Cyclodextrin stabilized freeze-dried silica/chitosan nanoparticles for improved terconazole ocular bioavailability. *Pharmaceutics* **14**. https://doi.org/10.3390/pharmaceutics14030470

Zainol Abidin N A, Kormin F, Zainol Abidin N A, Bakar M F A and Moujdin I A (2023) Synthesis and characterization of curcumin-chitosan loaded gold nanoparticles by *Oryctes rhinoceros*' chitin for cosmeceutical application. *Molecules* **28**. https://doi.org/10.3390/molecules28041799

Zakaria M Y, Fayad E, Althobaiti F, Zaki I and Abu Almaaty A H (2021) Statistical optimization of bile salt deployed nanovesicles as a potential platform for oral delivery of piperine: accentuated antiviral and anti-inflammatory activity in MERS-CoV challenged mice. *Drug Deliv.* **28**, 1150-1165. https://doi.org/10.1080/10717544.2021.1934190

Zeeshan M, Ain Q U, Sunny A, Raza F, Mohsin M, Khan S, Weigmann B and Ali H (2023) QbD-based fabrication of transferrin-anchored nanocarriers for targeted drug delivery to macrophages and colon cells for mucosal inflammation healing. *Biomater. Sci.* **11**, 1373-1397. https://doi.org/10.1039/d2bm01719a